

# Structured Sparsity of Convolutional Neural Networks via Nonconvex Sparse Group Regularization

Kevin Bui<sup>1</sup>, Fredrick Park<sup>2</sup>, Shuai Zhang<sup>1</sup>, Yingyong Qi<sup>1</sup>, and Jack Xin<sup>1,\*</sup>

<sup>1</sup>*Department of Mathematics; University of California, Irvine; Irvine, CA 92697, United States*

<sup>2</sup>*Department of Mathematics & Computer Science; Whittier College; Whittier, CA 90602, United States*

Correspondence\*:  
Corresponding Author  
jack.xin@uci.edu

## 2 ABSTRACT

3 Convolutional neural networks (CNN) have been hugely successful recently with superior  
4 accuracy and performance in various imaging applications, such as classification, object detection,  
5 and segmentation. However, a highly accurate CNN model requires millions of parameters to be  
6 trained and utilized. Even to increase its performance slightly would require significantly more  
7 parameters due to adding more layers and/or increasing the number of filters per layer. Apparently,  
8 many of these weight parameters turn out to be redundant and extraneous, so the original, dense  
9 model can be replaced by its compressed version attained by imposing inter- and intra-group  
10 sparsity onto the layer weights during training. In this paper, we propose a nonconvex family of  
11 sparse group lasso that blends nonconvex regularization (e.g., transformed  $\ell_1$ ,  $\ell_1 - \ell_2$ , and  $\ell_0$ )  
12 that induces sparsity onto the individual weights and  $\ell_{2,1}$  regularization onto the output channels  
13 of a layer. We apply variable splitting onto the proposed regularization to develop an algorithm  
14 that consists of two steps per iteration: gradient descent and thresholding. Numerical experiments  
15 are demonstrated on various CNN architectures showcasing the effectiveness of the nonconvex  
16 family of sparse group lasso in network sparsification and test accuracy on par with the current  
17 state of the art.

18 **Keywords:** deep learning, sparsity, nonconvex optimization, sparse group lasso, feature selection

## 1 INTRODUCTION

19 Deep neural networks (DNNs) have proven to be advantageous for numerous modern computer vision  
20 tasks involving image or video data. In particular, convolutional neural networks (CNNs) yield highly  
21 accurate models with applications in image classification [39, 77, 28, 95], semantic segmentation [49, 13],  
22 and object detection [73, 30, 72]. These large models often contain millions of weight parameters that often  
23 exceed the number of training data. This is a double-edged sword since on one hand, large models allow for  
24 high accuracy, while on the other, they contain many redundant parameters that lead to overparametrization.

25 Overparametrization is a well-known phenomenon in DNN models [17, 6] that results in overfitting,  
26 learning useless random patterns in data [96], and having inferior generalization. Additionally, these  
27 models also possess exorbitant computational and memory demands during both training and inference.  
28 Consequently, they may not be applicable for devices with low computational power and memory.

29 Resolving these problems requires compressing the networks through sparsification and pruning.  
30 Although removing weights might affect the accuracy and generalization of the models, previous  
31 works [54, 25, 81, 66] demonstrated that many networks can be substantially pruned with negligible  
32 effect on accuracy. There are many systematic approaches to achieving sparsity in DNNs, as discussed  
33 extensively in [14, 15].

34 Han *et al.* [26] proposed to first train a dense network, prune it afterward by setting the weights to zeroes  
35 if below a fixed threshold, and retrain the network with the remaining weights. Jin *et al.* [32] extended this  
36 method by restoring the pruned weights, training the network again, and repeating the process. Rather  
37 than pruning by thresholding, Aghasi *et al.* [1, 2] proposed Net-Trim, which prunes an already trained  
38 network layer by layer using convex optimization in order to ensure that the layer inputs and outputs remain  
39 consistent with the original network. For CNNs in particular, filter or channel pruning is preferred because  
40 it significantly reduces the amount of weight parameters required compared to individual weight pruning.  
41 Li *et al.* [43] calculated the sums of absolute weights of the filters of each layer and pruned the ones  
42 with the smallest sums. Hu *et al.* [29] proposed a metric called average percentage of zeroes for channels  
43 to measure their redundancies and pruned those with highest values for each layer. Zhuang *et al.* [105]  
44 developed discrimination-aware channel pruning that selects channels that contribute to the network's  
45 discriminative power.

46 An alternative approach to pruning a dense network is learning a compressed structure from scratch. A  
47 conventional approach is to optimize the loss function equipped with either the  $\ell_1$  or  $\ell_2$  regularization,  
48 which drives the weights to zeroes or to very small values during training. To learn which groups of weights  
49 (e.g., neurons, filters, channels) are necessary, group regularization, such as group lasso [93] and sparse  
50 group lasso [76], are equipped to the loss function. Alvarez and Salzmann [4] and Scardapane *et al.* [75]  
51 applied group lasso and sparse group lasso to various architectures and obtained compressed networks  
52 with comparable or even better accuracy. Instead of sharing features among the weights as suggested by  
53 group sparsity, exclusive sparsity [104] promotes competition for features between different weights. This  
54 method was investigated by Yoon and Hwang [92]. In addition, they combined it with group sparsity and  
55 demonstrated that this combination resulted in compressed networks with better performance than their  
56 original counterparts. Non-convex regularization has also been examined. Louizos *et al.* [54] proposed  
57 a practical algorithm using probabilistic methods to perform  $\ell_0$  regularization on CNNs. Ma *et al.* [61]  
58 proposed integrated transformed  $\ell_1$ , a convex combination of transformed  $\ell_1$  and group lasso, and compared  
59 its performance against the aforementioned group regularization methods.

60 In this paper, we propose a family of group regularization methods that balances both group lasso for  
61 group-wise sparsity and nonconvex regularization for element-wise sparsity. The family extends sparse  
62 group lasso by replacing the  $\ell_1$  penalty term with a nonconvex penalty term. The nonconvex penalty terms  
63 considered are  $\ell_0$ ,  $\ell_1 - \alpha\ell_2$ , transformed  $\ell_1$ , and SCAD. The proposed family is supposed to yield a more  
64 accurate and/or more compressed network than sparse group lasso since  $\ell_1$  suffers various weaknesses due  
65 to being a convex relaxation of  $\ell_0$ . We develop an algorithm to optimize loss functions equipped with the  
66 proposed nonconvex, group regularization terms for DNNs.

## 2 MODEL AND ALGORITHM

### 67 2.1 Preliminaries

Given a training dataset consisting of  $N$  input-output pairs  $\{(x_i, y_i)\}_{i=1}^N$ , the weight parameters of a DNN are learned by optimizing the following objective function:

$$\min_W \frac{1}{N} \sum_{i=1}^N \mathcal{L}(h(x_i, W), y_i) + \lambda \mathcal{R}(W), \quad (1)$$

68 where

- 69 •  $W$  is the set of weight parameters of the DNN.
- 70 •  $h(\cdot, \cdot)$  is the output of the DNN used for prediction.
- 71 •  $\mathcal{L}(\cdot, \cdot) \geq 0$  is the loss function that compares the prediction  $h(x_i, W)$  with the ground-truth output  $y_i$ .
- 72 Examples include cross-entropy loss function for classification and mean-squared error for regression.
- 73 •  $\mathcal{R}(\cdot)$  is the regularizer on the set of weight parameters  $W$ .
- 74 •  $\lambda > 0$  is a regularization parameter for  $\mathcal{R}(\cdot)$ .

75 The most common regularizer used for DNNs is  $\ell_2$  regularization  $\|\cdot\|_2^2$ , also known as weight decay. It  
 76 prevents overfitting and improves generalization because it enforces the weights to decrease proportionally  
 77 to their magnitudes [40]. Sparsity can be imposed by pruning weights whose magnitudes are below a  
 78 certain threshold at each iteration during training. However, an alternative regularizer is the  $\ell_1$  norm  
 79  $\|\cdot\|_1$ , also known as the lasso penalty [78]. The  $\ell_1$  norm is the tightest convex relaxation of the  $\ell_0$   
 80 penalty [20, 23, 82] and it yields a sparse solution that is found on the corners of the 1-norm ball [27, 52].  
 81 Theoretical results justify the  $\ell_1$  norm's ability to reconstruct sparse solution in compressed sensing. When  
 82 a sensing matrix satisfies the restricted isometry property, the  $\ell_1$  norm recovers the sparse solution exactly  
 83 with high probability [11, 23, 82]. On the other hand, the null space property is a necessary and sufficient  
 84 condition for  $\ell_1$  minimization to guarantee exact recovery of sparse solutions [16, 23]. Being able to  
 85 yield sparse solutions, the  $\ell_1$  norm has gained popularity in other types of inverse problems such as  
 86 compressed imaging [33, 57] and image segmentation [35, 34, 42] and in various fields of applications  
 87 such as geoscience [74], medical imaging [33, 57], machine learning [10, 78, 36, 67, 89], and traffic flow  
 88 network [91]. Unfortunately, element-wise sparsity by  $\ell_1$  or  $\ell_2$  regularization in CNNs may not yield  
 89 meaningful speedup as the number of filters and channels required for computation and inference may  
 90 remain the same [86].

To determine which filters or channels are relevant in each layer, group sparsity using the group lasso  
 penalty [93] is considered. The group lasso penalty has been utilized in various applications, such as  
 microarray data analysis [62], machine learning [7, 65], and EEG data [46]. Suppose a DNN has  $L$  layers,  
 so the set of weight parameters  $W$  is divided into  $L$  sets of weights:  $W = \{W_l\}_{l=1}^L$ . The weight set of each  
 layer  $W_l$  is divided into  $N_l$  groups (e.g., channels or filters):  $W_l = \{w_{l,g}\}_{g=1}^{N_l}$ . The group lasso penalty  
 applied to  $W_l$  is formulated as

$$\mathcal{R}_{GL}(W_l) = \sum_{g=1}^{N_l} \sqrt{\#w_{l,g}} \|w_{l,g}\|_2 = \sum_{g=1}^{N_l} \sqrt{\#w_{l,g}} \sqrt{\sum_{i=1}^{\#w_{l,g}} w_{l,g,i}^2}, \quad (2)$$

91 where  $w_{l,g,i}$  corresponds to the weight parameter with index  $i$  in group  $g$  in layer  $l$  and the term  $\#w_{l,g}$   
 92 denotes the number of weight parameters in group  $g$  in layer  $l$ . Because group sizes vary, the constant  
 93  $\sqrt{\#w_{l,g}}$  is multiplied in order to rescale the  $\ell_2$  norm of each group with respect to the group size, ensuring  
 94 that each group is weighed uniformly [93, 76, 65]. The group lasso regularizer imposes the  $\ell_2$  norm on  
 95 each group, forcing weights of the same groups to decrease altogether at every iteration during training. As  
 96 a result, the groups of weights are pruned when their  $\ell_2$  norms are negligible, resulting in a highly compact  
 97 network compared to element-sparse networks.

As an alternative to group lasso that encourages feature sharing, exclusive sparsity [104] enforces the model weight parameters to compete for features, making the features discriminative for each class in the context of classification. The regularization for exclusive sparsity is

$$\frac{1}{2} \sum_{g=1}^{N_l} \|w_{l,g}\|_1^2 = \frac{1}{2} \sum_{g=1}^{N_l} \left( \sum_{i=1}^{\#w_{l,g}} |w_{l,g,i}| \right)^2. \quad (3)$$

Now, within each group, sparsity is enforced. Because exclusivity cannot guarantee the optimal features since some features do need to be shared, exclusive sparsity can be combined with group sparsity to form combined group and exclusive sparsity (CGES) [92]. CGES is formulated as

$$\mathcal{R}_{CGES} = \sum_{g=1}^{N_l} \left[ (1 - \mu_l) \sqrt{\sum_{i=1}^{\#w_{l,g}} w_{l,g,i}^2} + \frac{\mu_l}{2} \left( \sum_{i=1}^{\#w_{l,g}} |w_{l,g,i}| \right)^2 \right], \quad (4)$$

98 where  $\mu_l \in (0, 1)$  is a parameter for balancing exclusivity and sharing among features.

To obtain an even sparser network, element-wise sparsity and group sparsity can be combined and applied together to the training of DNNs. One regularizer that combines these two types of sparsity is the sparse group lasso penalty [76], which is formulated as

$$\mathcal{R}_{SGL_1}(W_l) = \mathcal{R}_{GL}(W_l) + \|W_l\|_1 \quad (5)$$

where

$$\|W_l\|_1 = \sum_{g=1}^{N_l} \sum_{i=1}^{\#w_{l,g}} |w_{l,g,i}|.$$

99 Sparse group lasso simultaneously enforces group sparsity by having the regularizer  $\mathcal{R}_{GL}(\cdot)$  and  
 100 element-wise sparsity by having the  $\ell_1$  norm. This regularizer has been used in machine learning [83],  
 101 bioinformatics [48, 103], and medical imaging [47].

102 Figure 1 demonstrates the differences between lasso, group lasso, and sparse group lasso applied to a  
 103 weight matrix connecting a 5-dimensional input layer to a 10-dimensional output layer. In white, the entries  
 104 are zero'ed out; in gray; the entries are not. Unlike lasso, group lasso results in a more structured method  
 105 of pruning since three of the five neurons can be zero'ed out. Combined with  $\ell_1$  regularization on the  
 106 individual weights, sparse group lasso allows for more weights in the remaining two neurons to be pruned.

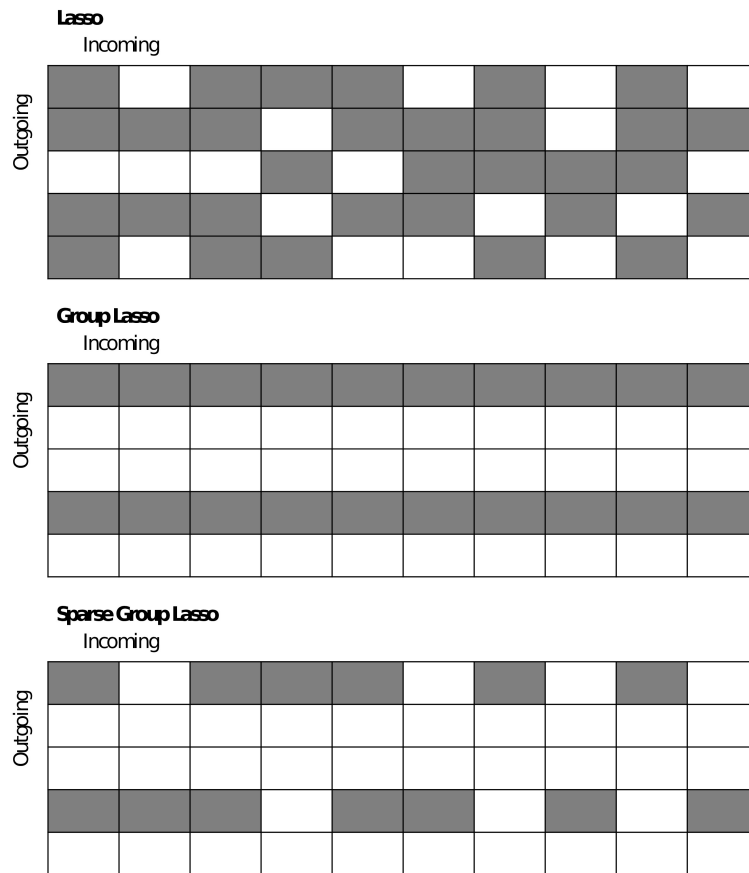


**Figure 1.** Comparison between lasso, group lasso, and sparse group lasso applied to a weight matrix. Entries in white are zero'ed out or removed; entries in gray remain.

107 **2.2 Nonconvex Sparse Group Lasso**

We recall that the  $\ell_1$  norm is the tightest convex relaxation of the  $\ell_0$  penalty, given by

$$\|W_l\|_0 = \sum_{g=1}^{N_l} \sum_{i=1}^{\#w_{l,g}} |w_{l,g,i}|_0 \tag{6}$$

where

$$|w|_0 = \begin{cases} 1 & \text{if } w \neq 0 \\ 0 & \text{if } w = 0 \end{cases}$$

108 when applied to the weight set  $W_l$  of layer  $l$ . The  $\ell_0$  penalty is non-convex and discontinuous. In addition,  
 109 any  $\ell_0$ -regularized problem is NP-hard [23]. These properties make developing convergent and tractable  
 110 algorithms for  $\ell_0$ -regularized problems difficult, thereby making  $\ell_1$ -regularized problems better alternatives  
 111 to solve. However, the  $\ell_0$ -regularized problems have been shown to recover better solutions in terms of  
 112 sparsity and/or accuracy than do  $\ell_1$ -regularized problems in various applications, such as compressed  
 113 sensing [56], image restoration [8, 12, 19, 102, 55], MRI reconstruction [80], and machine learning [56, 94].  
 114 In particular,  $\ell_0$ -regularized inverse problems were demonstrated to be more robust against Poisson noise  
 115 than are  $\ell_1$ -regularized inverse problems [100].

A continuous alternative to the  $\ell_0$  penalty is the SCAD penalty term [22, 58], given by

$$\lambda \|W_l\|_{\text{SCAD}(a)} = \sum_{g=1}^{N_l} \sum_{i=1}^{\#w_{l,g}} \lambda |w_{l,g,i}|_{\text{SCAD}(a)} \quad (7)$$

where

$$\lambda |w|_{\text{SCAD}(a)} := \begin{cases} \lambda |w| & \text{if } |w| < \lambda \\ \frac{2a\lambda|w| - w^2 - \lambda^2}{2(a-1)} & \text{if } \lambda \leq |w| < a\lambda \\ (a+1)\lambda^2/2 & \text{if } |w| \geq a\lambda \end{cases}$$

116 for  $\lambda > 0$  and  $a > 2$ . This penalty term enjoys three properties – unbiasedness, sparsity, and continuity  
 117 – while the  $\ell_1$  norm, on the other hand, has only sparsity and continuity [22]. In linear and logistic  
 118 regression, SCAD was shown to outperform  $\ell_1$  in variable selection [22]. SCAD has been applied to  
 119 wavelet approximation [5], bioinformatics [9, 84], and compressed sensing [64].

The transformed  $\ell_1$  penalty term [68] also enjoys the properties of unbiasedness, sparsity, and continuity [58]. In fact, the regularizer is not just continuous but Lipschitz continuous [98]. The term is given by

$$\|W_l\|_{\text{TL1}(a)} = \sum_{g=1}^{N_l} \sum_{i=1}^{\#w_{l,g}} |w_{l,g,i}|_{\text{TL1}(a)} \quad (8)$$

where

$$|w|_{\text{TL1}(a)} = \frac{(a+1)|w|}{a+|w|}.$$

In addition, it interpolates the  $\ell_0$  and  $\ell_1$  penalties through the parameter  $a$  [98] because

$$\lim_{a \rightarrow 0^+} |w|_{\text{TL1}(a)} = |w|_0 \quad \text{and} \quad \lim_{a \rightarrow \infty} |w|_{\text{TL1}(a)} = |w|.$$

120 The transformed  $\ell_1$  penalty term was investigated and was shown to outperform  $\ell_1$  in compressed  
 121 sensing [97, 98, 79], deep learning [61, 87, 45], matrix completion [99], and epidemic forecasting [45].

Another Lipschitz continuous, nonconvex regularizer is the  $\ell_1 - \alpha\ell_2$  penalty given by

$$\|W_l\|_{\ell_1 - \alpha\ell_2} = \|W_l\|_1 - \alpha\|W_l\|_2 = \sum_{g=1}^{N_l} \sum_{i=1}^{\#w_{l,g}} |w_{l,g,i}| - \alpha \sqrt{\sum_{g=1}^{N_l} \sum_{i=1}^{\#w_{l,g}} |w_{l,g,i}|^2}, \tag{9}$$

122 where  $\alpha \in (0, 1]$ . In a series of works [52, 90, 50, 51], the penalty term  $\ell_1 - \ell_2$  with  $\alpha = 1$  yields better  
 123 solutions than does  $\ell_1$  in various compressed sensing applications especially when the sensing matrix is  
 124 highly coherent or it violates the restricted isometry property condition. To guarantee exact recovery of  
 125 sparse solution,  $\ell_1 - \ell_2$  only requires a relaxed variant of the null space property [79]. Furthermore,  $\ell_1 - \alpha\ell_2$   
 126 is more robust against impulsive noise in yielding sparse, accurate solutions for inverse problems than is  
 127  $\ell_1$  [44]. Besides compressed sensing, it has been utilized in image denoising and deblurring [53], image  
 128 segmentation [71], image inpainting [63], and hyperspectral demixing [21]. In deep learning application,  
 129 the  $\ell_1 - \ell_2$  regularization was used to learn permutation matrices [59] for ShuffleNet [101, 60].

130 Due to the advantages and recent successes of the aforementioned nonconvex regularizers, we propose to  
 131 replace the  $\ell_1$  norm in (5) with nonconvex penalty terms. Hence, we propose a family of group regularizers  
 132 called nonconvex sparse group lasso. The family includes the following:

$$\mathcal{R}_{SGL_0}(W_l) = \mathcal{R}_{GL}(W_l) + \|W_l\|_0 \tag{10}$$

$$\mathcal{R}_{SGSCAD(a)}(W_l) = \mathcal{R}_{GL}(W_l) + \|W_l\|_{SCAD(a)} \tag{11}$$

$$\mathcal{R}_{SGTL_1(a)}(W_l) = \mathcal{R}_{GL}(W_l) + \|W_l\|_{TL_1(a)} \tag{12}$$

$$\mathcal{R}_{SGL_1 - \alpha L_2}(W_l) = \mathcal{R}_{GL}(W_l) + \|W_l\|_{\ell_1 - \alpha\ell_2}. \tag{13}$$

133 Using these regularizers, we expect to obtain a sparser and/or more accurate network than from using  
 134 the original sparse group lasso. The  $\ell_1$  norm can also be replaced with other nonconvex penalties not  
 135 mentioned in this paper. Refer to [3, 85] to see other nonconvex penalties. However, we focus on the  
 136 aforementioned nonconvex regularizers because they have closed-form proximal operators required by our  
 137 proposed algorithm described in the next section.

### 138 2.3 Notations and Definitions

139 Before discussing the algorithm, we summarize notations that we will use to save space. They are the  
 140 following:

- 141 • If  $V = \{V_l\}_{l=1}^L$  and  $W = \{W_l\}_{l=1}^L$ , then  $(V, W) := (\{V_l\}_{l=1}^L, \{W_l\}_{l=1}^L) =$   
 142  $(V_1, \dots, V_L, W_1, \dots, W_L)$ .
- 143 •  $V^+ := V^{k+1}$ .
- 144 •  $\tilde{\mathcal{L}}(W) := \frac{1}{N} \sum_{i=1}^N \mathcal{L}(h(x_i, W), y_i)$ .

In addition, we define the proximal operator for the regularization function  $r(\cdot)$  as follows:

$$\text{prox}_{\lambda r}(y) = \arg \min_x \lambda r(x) + \frac{1}{2} \|x - y\|_2^2$$

145 for  $\lambda > 0$ .

## 146 2.4 Numerical Optimization

We develop a general algorithm framework to solve

$$\min_W \tilde{\mathcal{L}}(W) + \lambda \sum_{l=1}^L \mathcal{R}(W_l) = \tilde{\mathcal{L}}(W) + \sum_{l=1}^L (\lambda \mathcal{R}_{GL}(W_l) + \lambda r(W_l)) \quad (14)$$

147 where  $W = \{W_l\}_{l=1}^L$ ,  $\mathcal{R}$  is either  $\mathcal{R}_{SGL_1}$  or one of the nonconvex regularizers (10)-(13), and  $r(\cdot)$  is the  
148 corresponding sparsity-inducing regularizer. Throughout the paper, our assumption on (14) is the following:

149 **ASSUMPTION 1.** *The function  $\tilde{\mathcal{L}}$  is continuously differentiable with respect to  $W_l$  for each  $l = 1, \dots, L$ .*

150 By introducing an auxiliary variable  $V = \{V_l\}_{l=1}^L$  for (14), we have a constrained optimization problem:

$$\begin{aligned} \min_{V, W} \quad & \tilde{\mathcal{L}}(W) + \sum_{l=1}^L (\lambda \mathcal{R}_{GL}(W_l) + \lambda r(V_l)) \\ \text{s.t.} \quad & V_l = W_l \quad l = 1, \dots, L. \end{aligned} \quad (15)$$

151 The constraints can be relaxed by adding the quadratic penalty terms with  $\beta > 0$  so that we have

$$\min_{V, W} F_\beta(V, W) := \tilde{\mathcal{L}}(W) + \sum_{l=1}^L \left[ \lambda \mathcal{R}_{GL}(W_l) + \lambda r(V_l) + \frac{\beta}{2} \|V_l - W_l\|_2^2 \right]. \quad (16)$$

With  $\beta$  fixed, (16) can be solved by alternating minimization:

$$W^{k+1} = \arg \min_W F_\beta(V^k, W) \quad (17a)$$

$$V^{k+1} = \arg \min_V F_\beta(V, W^{k+1}). \quad (17b)$$

To solve (17a), we simultaneously update  $W_l$  for  $l = 1, \dots, L$  by gradient descent

$$W_l^{k+1} = W_l^k - \gamma \left( \nabla_{W_l} \tilde{\mathcal{L}}(W^k) + \lambda \partial_{W_l} \mathcal{R}_{GL}(W_l^k) - \beta (V_l^k - W_l^k) \right) \quad (18)$$

152 where  $\gamma > 0$  is the learning rate and  $\partial_{W_l} \mathcal{R}_{GL}$  is the subdifferential of  $\mathcal{R}_{GL}$  with respect to  $W_l$ . In practice,  
153 (18) is performed using stochastic gradient descent (or one of its variants) with mini-batches due to the  
154 large-size computation dealing with the amount of data and weight parameters that a typical DNN has.

To update  $V$ , we see that (17b) can be rewritten as

$$V^{k+1} = \arg \min_V \sum_{l=1}^L \left( \frac{\lambda}{\beta} r(V_l) + \frac{1}{2} \|V_l - W_l\|_2^2 \right) = \left( \text{prox}_{\frac{\lambda}{\beta} r}(W_1), \dots, \text{prox}_{\frac{\lambda}{\beta} r}(W_L) \right). \quad (19)$$

155 The proximal operators for the considered regularizers are thresholding functions as their closed-form  
156 solutions, and as a result, the  $V$  update simplifies to thresholding  $W$ . The regularization functions and their  
157 corresponding proximal operators are summarized in Table 1.



**Algorithm 1:** Algorithm for Nonconvex Sparse Group Lasso Regularization

---

```

1 Initialize  $V^1$  and  $W^1$  with random entries; learning rate  $\gamma$ ; regularization parameters  $\lambda$  and  $\beta$ ; and
  multiplier  $\sigma > 1$ .
2 Set  $j := 1$ .
3 while stopping criterion for outer loop not satisfied do
4   Set  $k := 1$ .
5   Set  $W^{j,1} = W^j$  and  $V^{j,1} = V^j$ .
6   while stopping criterion for inner loop not satisfied do
7     Update  $W^{j,k+1}$  by Eq. (18).
8     Update  $V^{j,k+1}$  by Eq. (19).
9      $k := k + 1$ 
10  end
11  Set  $W^{j+1} = W^{j,k}$  and  $V^{j+1} = V^{j,k}$ .
12  Set  $\beta := \sigma\beta$ .
13  Set  $j := j + 1$ .
14 end
15 Output:  $W^j$  and  $V^j$ .

```

---

158 Incorporating the algorithm that solves the quadratic penalty problem (16), we now develop a general  
 159 algorithm to solve (14). We solve a sequence of quadratic penalty problems (16) with  $\beta \in \{\beta_j\}_{j=1}^{\infty}$  where  
 160  $\beta_j \uparrow \infty$ . This will yield a sequence  $\{(V^j, W^j)\}_{j=1}^{\infty}$  so that  $W^j \uparrow W^*$ , a solution to (14). This algorithm is  
 161 based on the quadratic penalty method [69] and the penalty decomposition method [56]. The algorithm is  
 162 summarized in Algorithm 1.

An alternative algorithm to solve (14) is proximal gradient descent [70]. By this method, the update for  $W_l, l = 1, \dots, L$ , is

$$W_l^{k+1} = \text{prox}_{\gamma\lambda r} \left( W_l^k - \gamma \left( \nabla_{W_l} \tilde{\mathcal{L}}(W^k) + \lambda \partial_{W_l} \mathcal{R}_{GL}(W_l^k) \right) \right). \quad (20)$$

163 Using this algorithm results in weight parameters with some already zero'ed out.

However, the advantage of our proposed algorithm lies in (17a), written more specifically as

$$\begin{aligned} W_l^{k+1} &= \arg \min_{W_l} \tilde{\mathcal{L}}(W) + \mathcal{R}_{GL}(W_l) + \frac{\beta}{2} \|V_l - W_l\|_2^2 \\ &= \arg \min_{W_l} \tilde{\mathcal{L}}(W) + \mathcal{R}_{GL}(W_l) + \frac{\beta}{2} \sum_{i=1}^{\#W_l} (v_{l,i} - w_{l,i})^2. \end{aligned} \quad (21)$$

164 We see that this step performs exact weight decay or  $\ell_2$  regularization on weights  $w_{l,i}$  whenever  $v_{l,i} = 0$ .  
 165 On the other hand, when  $v_{l,i} \neq 0$ , the effect of  $\ell_2$  regularization is mitigated on the corresponding weight  
 166  $w_{l,i}$  based on the absolute difference  $|v_{l,i} - w_{l,i}|$ . Using  $\ell_2$  regularization was shown to give superior  
 167 pruning results in terms of accuracy by Han et al. [26]. Our proposed algorithm can be perceived as an  
 168 adaptive  $\ell_2$  regularization method, where (17b) identifies which weights to perform exact  $\ell_2$  regularization  
 169 on and (17a) updates and regularizes the weights accordingly.

170

## 171 2.5 Convergence Analysis

172 To establish convergence for the proposed algorithm, the results below state that the accumulation  
 173 point of the sequence generated by (17a)-(17b) is a block-coordinate minimizer, and an accumulation  
 174 point generated by Algorithm 1 is a sparse feasible solution to (15). Proofs are provided in Section 5.  
 175 Unfortunately, the feasible solution generated may not be a local minimizer of (15) because the loss  
 176 function  $\mathcal{L}(\cdot, \cdot)$  is nonconvex. However, it was shown in [18] that a similar algorithm to Algorithm 1, but  
 177 for fixed  $\beta$  in a bounded interval, generates an approximate global solution with high probability for a  
 178 one-layer CNN with ReLu activation function.

**THEOREM 2.** *Let  $\{(V^k, W^k)\}_{k=1}^{\infty}$  be a sequence generated by the alternating minimization algorithm (17a)-(17b), where  $r(\cdot)$  is  $\ell_0$ ,  $\ell_1$ , transformed  $\ell_1$ ,  $\ell_1 - \alpha\ell_2$ , or SCAD. If  $(V^*, W^*)$  is an accumulation point of  $\{(V^k, W^k)\}_{k=1}^{\infty}$ , then  $(V^*, W^*)$  is a block-coordinate minimizer of (16). that is*

$$V^* \in \arg \min_V F_{\beta}(V, W^*)$$

$$W^* \in \arg \min_W F_{\beta}(V^*, W).$$

179 **THEOREM 3.** *Let  $\{(V^k, W^k, \beta_k)\}_{k=1}^{\infty}$  be a sequence generated by Algorithm 1. Suppose that  
 180  $\{F_{\beta_k}(V^k, W^k)\}_{k=1}^{\infty}$  is uniformly bounded. If  $(V^*, W^*)$  is an accumulation point of  $\{(V^k, W^k)\}_{k=1}^{\infty}$ , then  
 181  $(V^*, W^*)$  is a feasible solution to (15), that is  $V^* = W^*$ .*

*Remark:* To safely ensure that  $\{F_{\beta_k}(V^k, W^k)\}_{k=1}^{\infty}$  is uniformly bounded in practice, we can find a feasible solution  $(V^{\text{feas}}, W^{\text{feas}})$  to (15) and impose a bound  $M$  such that

$$M \geq \max \left\{ \tilde{L}(W^{\text{feas}}) + \lambda \sum_{l=1}^L \mathcal{R}(W_l^{\text{feas}}), \min_W F_{\beta_0}(V^1, W) \right\}.$$

182 If  $\min_W F_{\beta_{k+1}}(V^k, W) > M$ , then we set  $V^{k+1} = W^{\text{feas}}$ . This strategy is based on [56]. However, in our  
 183 numerical experiments, we have not yet encountered  $F_{\beta_k}(V^k, W^k)$  to diverge.

## 3 NUMERICAL EXPERIMENTS

### 184 3.1 Application to Deep Neural Networks

185 We compare the proposed nonconvex sparse group lasso against four other methods as baselines: group  
 186 lasso, sparse group lasso ( $SGL_1$ ), CGES proposed in [92], and the group variant of  $\ell_0$  regularization  
 187 (denoted as  $\ell_0$  for simplicity) proposed in [54].  $SGL_1$  is optimized using the same algorithm proposed  
 188 for nonconvex sparse group lasso. For the group terms, the weights are grouped together based on the  
 189 filters or output channels, which we will refer to as neurons. We trained various CNN architectures on  
 190 MNIST [41] and CIFAR 10/100 [38]. The MNIST dataset consists of 60k training images and 10k test  
 191 images. MNIST is trained on two simple CNN architectures: LeNet-5-Caffe [31, 41] and a 4-layer CNN  
 192 with two convolutional layers (32 and 64 channels, respectively) and an intermediate layer of 1000 fully  
 193 connected neurons. CIFAR 10/100 is a dataset that has 10/100 classes split into 50k training images and  
 194 10k test images. It is trained on Resnets [28] and wide Resnets [95]. Throughout all of our experiments, for  
 195  $SGSCAD(a)$ , we set  $a = 3.7$  as suggested in [22]; for  $SGTL_1(a)$ , we set  $a = 1.0$  as suggested in [99];  
 196 and for  $SGL_1 - L_2$ , we set  $\alpha = 1.0$  as suggested by the literatures [52, 90, 50, 51]. For CGES, we have  
 197  $\mu_l = l/L$ . Because the optimization algorithms do not drive most, if not all, the weights and neurons to

198 zeroes, we have to set them to zeroes when their values are below a certain threshold. In our experiments,  
199 if the absolute weights are below  $10^{-5}$ , we set them to zeroes. Then, **weight sparsity** is defined to be  
200 *the percentage of zero weights with respect to the total number of weights trained in the network*. If the  
201 normalized sum of the absolute values of the weights of the neuron is less than  $10^{-5}$ , then the weights of  
202 the neuron are set to zeroes. **Neuron sparsity** is defined to be *the percentage of neurons whose weights are*  
203 *zeroes with respect to the total number of neurons in the network*.

### 204 3.1.1 MNIST Classification

205 MNIST is trained on Lenet-5-Caffe, which has four layers with 1,370 total neurons and 431,080 total  
206 weight parameters. All layers of the network are applied with strictly the same type of regularization. No  
207 other regularization methods (e.g., dropout and batch normalization) are used. The network is optimized  
208 using Adam [37] with initial learning rate 0.001. For every 40 epochs, the learning rate decays by  
209 a factor of 0.1. We set the regularization parameter to the following values:  $\lambda = \alpha/60000$  for  $\alpha \in$   
210  $\{0.1, 0.2, 0.3, 0.4, 0.5\}$ . For  $SGL_1$  and nonconvex sparse group lasso, we set  $\beta = 25\alpha/60000$ , and for  
211 every 40 epochs,  $\beta$  increases by a factor of  $\sigma = 1.25$ . The network is trained for 200 epochs across 5 runs.

212 Table 2 reports the mean results for test error, weight sparsity, and neuron sparsity across five runs  
213 of Lenet-5-Caffe trained after 200 epochs. We see that although CGES has the lowest test errors at  
214  $\alpha \in \{0.1, 0.3, 0.4\}$  and the largest weight sparsity for all  $\alpha \in \{0.1, 0.2, \dots, 0.5\}$ , nonconvex sparse group  
215 lasso's test errors and weight sparsity are comparable. Additionally, nonconvex sparse group lasso's neuron  
216 sparsity is nearly two times larger than the neuron sparsity attained by CGES. Across all parameters and  
217 methods,  $SGL_0$  with  $\alpha = 0.5$  attains the best average test error of 0.630 with average weight sparsity 95.7%  
218 and neuron sparsity 80.7%. Furthermore, its test error is lower than the test errors of other nonconvex  
219 sparse group lasso regularization methods for all  $\alpha$ 's tested. Generally,  $SGL_1$  and nonconvex sparse group  
220 lasso outperform  $\ell_0$  regularization proposed by Louizos et al. [54] and group lasso by average weight and  
221 neuron sparsity.

222 Table 3 reports the mean results for test error, weight sparsity, and neuron sparsity of the Lenet-5-Caffe  
223 models with the lowest test errors from the five runs. According to the results, the best test errors are  
224 attained by  $SGL_0$  at  $\alpha = 0.3, 0.5$ ;  $SGL_1 - L_2$  at  $\alpha = 0.2$ ; and CGES at  $\alpha = 0.1, 0.4$ . For average  
225 weight sparsity,  $SGL_0$  attains the largest weight sparsity at  $\alpha \in \{0.2, 0.3, 0.4, 0.5\}$ . For average neuron  
226 sparsity, the largest values are attained by  $SGTL_1$  at  $\alpha = 0.1, 0.2$ ; by  $SGL_1$  at  $\alpha = 0.3$ ; and by  $SGL_0$  at  
227  $\alpha = 0.4, 0.5$ . Although  $SGL_0$  does not outperform all the other methods across the board, its results are  
228 still comparable to the best results. Overall, we see that nonconvex sparse group lasso outperforms  $\ell_0$  in  
229 test error, weight sparsity, and neuron sparsity and group lasso in weight and neuron sparsity.

230 MNIST is also trained on a 4-layer CNN with two convolutional layers with 32 and 64 channels,  
231 respectively, and an intermediate layer with 1000 neurons. Each convolutional layer has a  $5 \times 5$  convolutional  
232 filters. The 4-layer CNN has 2,120 total neurons and 1,087,010 total weight parameters. All layers of the  
233 network are applied with strictly the same type of regularization. The network is optimized with the same  
234 settings as Lenet-5-Caffe. However, the regularization parameter is different: we have  $\lambda = \alpha/60000$  for  
235  $\alpha \in \{0.2, 0.4, 0.6, 0.8, 1.0\}$ . For  $SGL_1$  and nonconvex sparse group lasso, we set  $\beta = 5\alpha/60000$  and for  
236 every 40 epochs,  $\beta$  increases by a factor of  $\sigma = 1.25$ . The network is trained for 200 epochs across 5 runs.

237 Table 4 reports the mean results for test error, weight sparsity, and neuron sparsity across five runs of  
238 the 4-layer CNN models trained after 200 epochs. Although CGES consistently has the highest weight  
239 sparsity, it does not yield the most accurate models until when  $\alpha \geq 0.8$ . Moreover, its neuron sparsity is  
240 smaller than the neuron sparsity by group lasso,  $SGL_1$ , and nonconvex group lasso when  $\alpha \geq 0.6$ .  $\ell_0$  has  
241 the highest neuron sparsity for all  $\alpha$ 's given, but its test errors are much greater. When  $\alpha \leq 0.6$ ,  $SGSCAD$

242 yields the most accurate models at  $\alpha = 0.2, 0.6$  while  $SGL_1$  yields one at  $\alpha = 0.4$ . Overall, we see that  
 243 nonconvex group lasso has comparable weight sparsity and neuron sparsity as group lasso and  $SGL_1$ .

244 Table 5 reports the mean results for test error, weight sparsity, and neuron sparsity of the 4-layer CNN  
 245 models with the lowest test errors from the five runs. At  $\alpha = 0.2$ ,  $SGL_1$  and  $SGSCAD$  have the lowest  
 246 test errors, but their weight sparsity are exceeded by CGES and their neuron sparsity are exceed by  $\ell_0$ . At  
 247  $\alpha = 0.4$ ,  $SGL_1 - L_2$  has the lowest test error, but its weight sparsity and neuron sparsity are exceeded  
 248 by CGES and  $\ell_0$ , respectively. At  $\alpha = 0.6$ ,  $SGL_1$  has the lowest test error, but  $SGSCAD$  has the largest  
 249 weight sparsity with comparable test error. At  $\alpha \geq 0.8$ , CGES has the lowest test error, but its weight  
 250 sparsity is exceeded by group lasso,  $SGL_1$ , and the nonconvex group lasso regularizers, which all have  
 251 slightly higher test error. At  $\alpha = 0.8$ , the neuron sparsity of CGES is comparable to the neuron sparsity of  
 252 group lasso,  $SGL_1$ , and the nonconvex group lasso regularizers. At  $\alpha = 1.0$ , group lasso has the highest  
 253 neuron sparsity, but nonconvex group lasso has slightly lower neuron sparsity. In general, weight sparsity  
 254 of nonconvex group lasso is comparable to or larger than the weight sparsity of group lasso and  $SGL_1$ .

### 255 3.1.2 CIFAR Classification

256 CIFAR 10/100 is trained on Resnet-40 and wide Resnet with depth 28 and width 10 (WRN-28-10). Resnet-  
 257 40 has approximately 570,000 weight parameters and 1520 neurons while WRN-28-10 has approximately  
 258 36,500,000 weight parameters and 10,736 neurons. The networks are optimized using stochastic gradient  
 259 descent with initial learning rate 0.1. After every 60 epochs, learning rate decays by a factor of 0.2.  
 260 Strictly the same type of regularization is applied to the weights of the hidden layer where dropout is  
 261 utilized in the residual block. We vary the regularization parameter  $\lambda = \alpha/50000$ . For Resnet-40, we have  
 262  $\alpha \in \{1.0, 1.5, 2.0, 2.5, 3.0\}$  for CIFAR 10 and  $\alpha \in \{2.0, 2.5, 3.0, 3.5, 4.0\}$  for CIFAR 100. For  $SGL_1$  and  
 263 nonconvex sparse group lasso, we set  $\beta = 15\alpha/50000$  for Resnet-40 and  $\beta = 25\alpha/50000$  for WRN-28-10.  
 264 For every 20 epochs,  $\beta$  increases by a factor of  $\sigma = 1.25$ . The networks are trained for 200 epochs across 5  
 265 runs. We excluded  $\ell_0$  regularization by Louizos *et al.* [54] because it was unstable for the provided  $\alpha$ 's.  
 266 Furthermore, we only analyze the models with the lowest test errors since the test errors did not stabilize  
 267 by the end of the 200 epochs in our experiments.

268 Table 6 reports mean test error, weight sparsity, and neuron sparsity across the Resnet-40 models trained  
 269 on CIFAR 10 with the lowest test errors from the five runs. Group lasso has the lowest test errors for all  
 270  $\alpha$ 's provided while CGES,  $SGL_1$ , and nonconvex sparse group lasso are higher by at most 1.1%. When  
 271  $\alpha \leq 1.5$ , CGES has the largest weight sparsity while  $SGSCAD$ ,  $SGTL_1$   $SGL_1 - SGL_2$  have larger  
 272 weight sparsity than does group lasso. At  $\alpha = 2.0, 2.5$ ,  $SGSCAD$  has the largest weight sparsity. At  
 273  $\alpha = 3.0$ ,  $SGL_1$  has the largest weight sparsity with comparable test error as the nonconvex group lasso  
 274 regularizers. For neuron sparsity,  $SGL_1 - L_2$  has the largest at  $\alpha = 1.0$  while  $SGSCAD$  has the largest  
 275 at  $\alpha = 1.5, 2.0$ . However, at  $\alpha = 2.5, 3.0$ , group lasso has the largest neuron sparsity. For all  $\alpha$ 's tested,  
 276  $SGSCAD$  has higher weight sparsity and neuron sparsity than does  $SGL_1$  but with comparable test error.

277 Table 7 reports mean test error, weight sparsity, and neuron sparsity across the Resnet-40 models trained  
 278 on CIFAR 100 with the lowest test errors from the five runs. Group lasso has the lowest test errors for  
 279  $\alpha \leq 3.5$  while CGES has the lowest test error at  $\alpha = 4.0$ . However, the weight sparsity and the neuron  
 280 sparsity of group lasso are lower than the sparsity of  $SGL_1$  and some of the nonconvex sparse group  
 281 lasso regularizers. CGES has the lowest neuron sparsity across all  $\alpha$ 's. Among the nonconvex group lasso  
 282 penalties,  $SGSCAD$  has the best test errors, which are lower than the test errors of  $SGL_1$  for all  $\alpha$ 's  
 283 except 2.5.

284 Table 8 reports mean test error, weight sparsity, and neuron sparsity across the WRN-28-10 models  
 285 trained on CIFAR 10 with the lowest test errors from the five runs. The best test errors are attained by

286  $SGTL_1$  at  $\alpha = 0.05, 0.2, 0.5$ ; by CGES at  $\alpha = 0.01$ ; and by  $SGL_1$  at  $\alpha = 0.1$ . Weight sparsity of CGES  
287 outperforms the other methods only when  $\alpha = 0.01, 0.05, 0.1$ , but it underperforms when  $\alpha \geq 0.2$ . Weight  
288 sparsity levels between group lasso and nonconvex group lasso are comparable across all  $\alpha$ . For neuron  
289 sparsity,  $SGL_1 - L_2$  attains the largest values at  $\alpha = 0.02, 0.1, 0.2$ . Nevertheless, the other nonconvex  
290 sparse group lasso methods have comparable neuron sparsity. Overall,  $SGL_1$ ,  $SGL_0$ ,  $SGSCAD$ , and  
291  $SGTL_1$  outperform group lasso in test error while having similar or higher weight and neuron sparsity.

292 Table 9 reports mean test error, weight sparsity, and neuron sparsity across the WRN-28-10 models  
293 trained on CIFAR 100 with the lowest test errors from the five runs. According to the results, the best  
294 test errors are attained by CGES when  $\alpha = 0.01, 0.05$ ; by  $SGSCAD$  when  $\alpha = 0.1, 0.5$ ; and by  $SGTL_1$   
295 when  $\alpha = 0.2$ . Although CGES has the largest weight sparsity for  $\alpha = 0.01, 0.05, 0.1, 0.2$ , we see that  
296 its test error increases as  $\alpha$  increases. When  $\alpha = 0.5$ , the best weight sparsity is attained by  $SGSCAD$ ,  
297 but the other methods have comparable weight sparsity. The best neuron sparsity is attained by CGES at  
298  $\alpha = 0.01, 0.02$ ; by  $SGL_1 - L_2$  at  $\alpha = 0.1, 0.2$ ; and by  $SGSCAD$  at  $\alpha = 0.5$ . The neuron sparsity among  
299 the nonconvex sparse group lasso methods are comparable. For  $\alpha \leq 0.2$ , we see that  $SGL_1$  and nonconvex  
300 sparse group lasso outperform group lasso in test error across  $\alpha$  while having comparable weight and  
301 neuron sparsity.

### 302 3.2 Algorithm Comparison

303 We compare the proposed Algorithm 1 with direct stochastic gradient descent, where the gradient of  
304 the regularizer is approximated by backpropagation, and proximal gradient descent, discussed in Section  
305 2.4, by applying them to  $SGL_1$  on Lenet-5 trained on MNIST. The parameter setting for this CNN is  
306 discussed in Section 3.1.1. Table 10 reports the mean results for test error, weight sparsity, and neuron  
307 sparsity across five models trained after 200 epochs while Figure 2 provides visualizations. Table 11 and  
308 Figure 3 record mean statistics for models with the lowest test errors from the five runs. According to  
309 the results, proximal stochastic gradient descent attains the highest level of weight sparsity and neuron  
310 sparsity for models trained after 200 epochs and models with the lowest test error. However, their test  
311 errors are the highest amongst the three algorithms. On the other hand, our proposed algorithm attains the  
312 lowest test errors. For models trained after 200 epochs, the weight sparsity and neuron sparsity attained  
313 by Algorithm 1 are comparable to the sparsity attained by direct stochastic gradient descent. For models  
314 with the lowest test errors generated from their respective runs, the weight sparsity and neuron sparsity  
315 by the proposed algorithm are better than the sparsity by direct stochastic gradient descent. Therefore,  
316 our proposed algorithm generates the most accurate model with satisfactory sparsity among the three  
317 algorithms for sparse regularization.

## 4 CONCLUSION AND FUTURE WORK

318 In this work, we propose nonconvex sparse group lasso, a nonconvex extension of sparse group lasso. The  
319  $\ell_1$  norm in sparse group lasso on the weight parameters is replaced with a nonconvex regularizer whose  
320 proximal operator is a thresholding function. Taking advantage of this property, we develop a new algorithm  
321 to optimize loss functions regularized with nonconvex sparse group lasso for CNNs in order to attain a  
322 sparse network with competitive accuracy. We compare the proposed family of regularizers with various  
323 baseline methods on MNIST and CIFAR 10/100 on different CNNs. The experimental results demonstrate  
324 that in general, nonconvex sparse group lasso generates a more accurate and/or more compressed CNN  
325 than does group lasso. In addition, we compare our proposed algorithm to direct stochastic gradient descent  
326 and proximal gradient descent on Lenet-5 trained on MNIST. The results show that the proposed algorithm  
327 to solve  $SGL_1$  yields a satisfactorily sparse network with lower test error than do the other two algorithms.

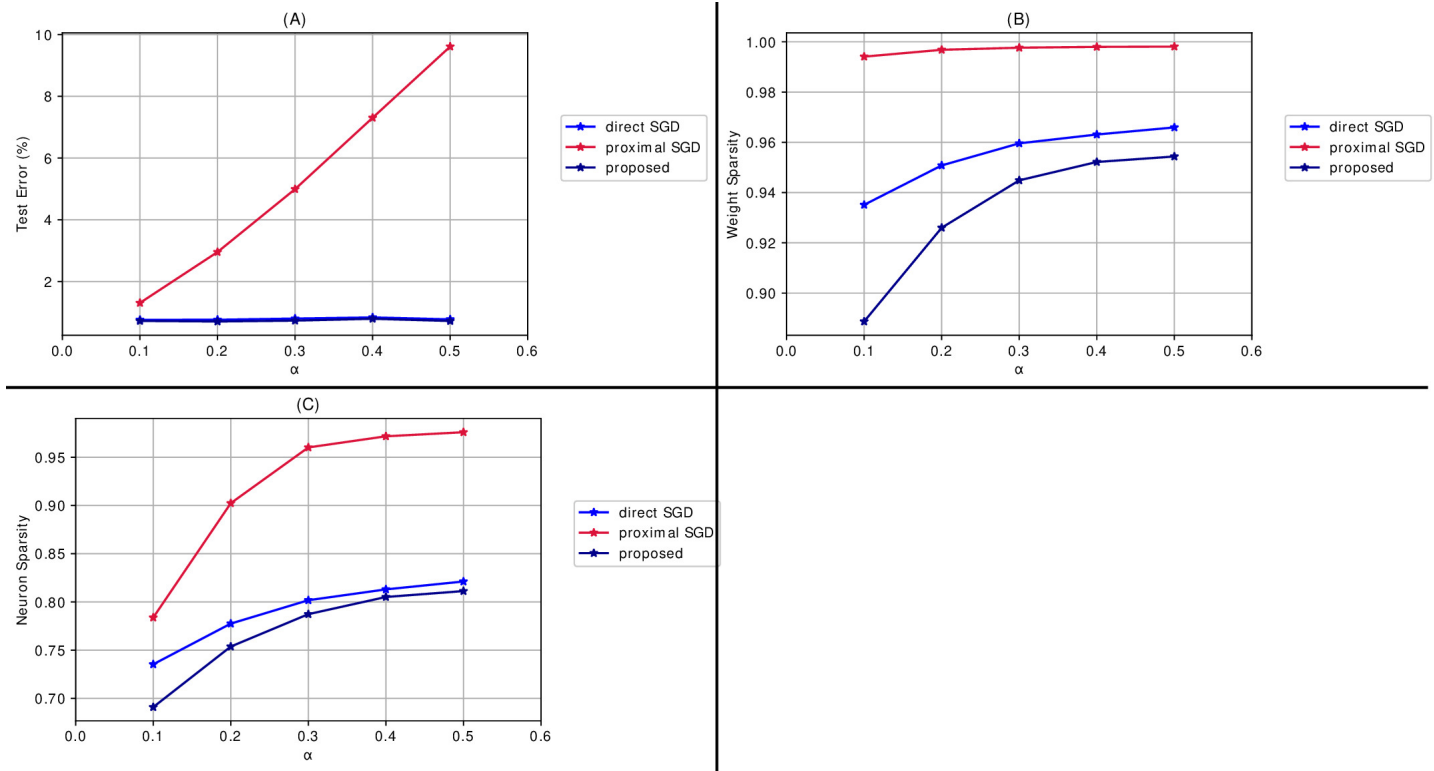


**Figure 2.** Mean results of algorithms applied to  $SGL_1$  for Lenet-5 models trained on MNIST for 200 epochs across 5 runs when varying the regularization parameter  $\lambda = \alpha/60000$  when  $\alpha \in \{0.1, 0.2, 0.3, 0.4, 0.5\}$ . (A) Mean test error. (B) Mean weight sparsity. (C) Mean neuron sparsity.

328 According to the numerical results, there is no single sparse regularizer that outperforms all other on any  
 329 CNN trained on a given dataset. One regularizer may perform well in one case while it may perform worse  
 330 on a different case. Due to the myriad of sparse regularizers to select from and the various parameters to  
 331 tune, especially for one CNN trained on a given dataset, one direction is to develop an automatic machine  
 332 learning framework that efficiently selects the right regularizer and parameters. In recent works, automatic  
 333 machine learning can be represented as a matrix completion problem [88] and a statistical learning problem  
 334 [24]. These frameworks can be adapted for selecting the best sparse regularizer, thus saving time for users  
 335 who are training sparse CNNs.

## 5 PROOFS

336 We provide proofs for the results discussed in Section 2.5.

### 337 5.1 Proof of Theorem 2

By (17a)-(17b), for each  $k \in \mathbb{N}$ , we have

$$F_\beta(V^k, W^{k+1}) \leq F_\beta(V^k, W) \quad (22)$$

for all  $W$ , and

$$F_\beta(V^{k+1}, W^{k+1}) \leq F_\beta(V, W^{k+1}) \quad (23)$$

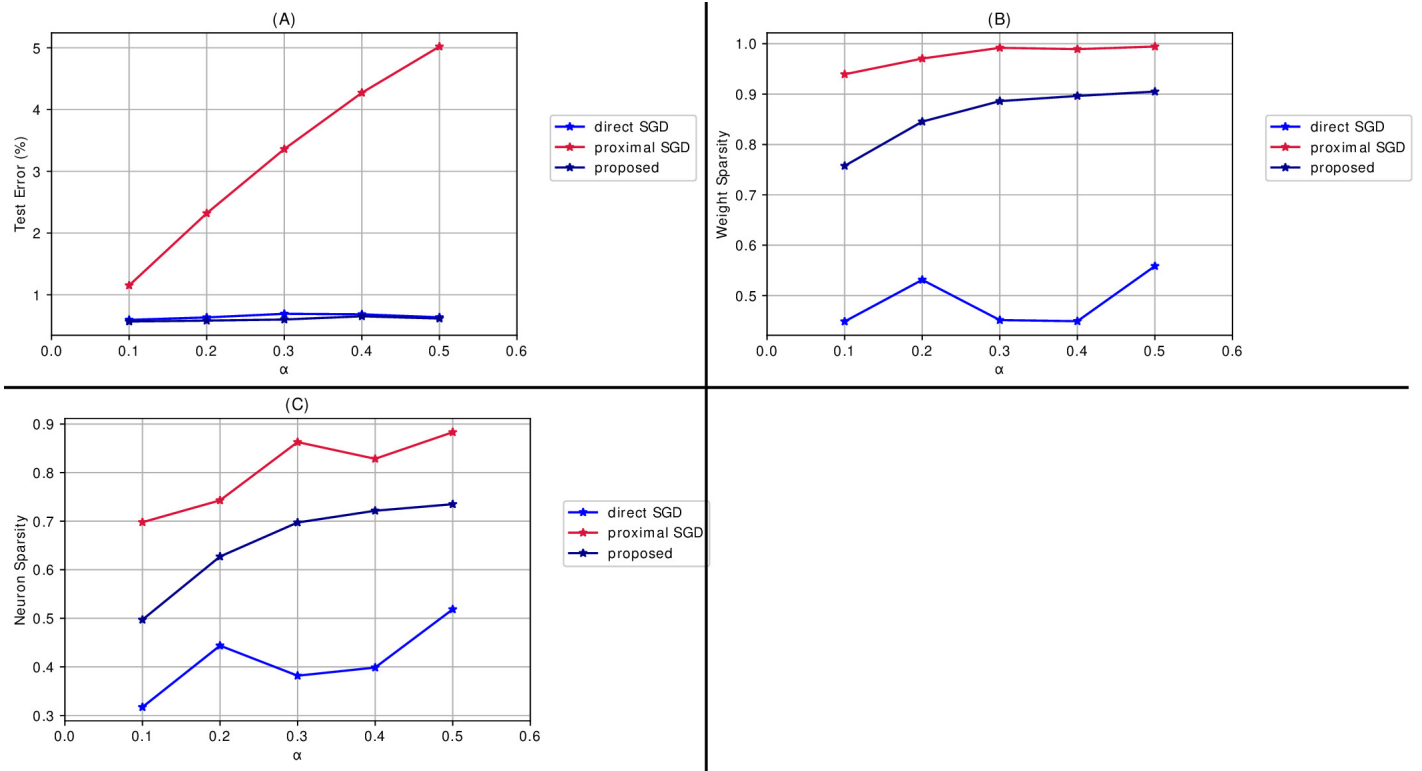


**Figure 3.** Mean results of algorithms applied to  $SGL_1$  for Lenet-5 models trained on MNIST with lowest test errors across 5 runs when varying the regularization parameter  $\lambda = \alpha/60000$  when  $\alpha \in \{0.1, 0.2, 0.3, 0.4, 0.5\}$ . (A) Mean test error. (B) Mean weight sparsity. (C) Mean neuron sparsity.

for all  $V$ . By (23), we have

$$F_\beta(V^+, W^+) \leq F_\beta(V^k, W^+) \tag{24}$$

for each  $k \in \mathbb{N}$ . Altogether, we have

$$F_\beta(V^+, W^+) \leq F_\beta(V^k, W^k) \tag{25}$$

for each  $k \in \mathbb{N}$ , so  $\{F_\beta(V^k, W^k)\}_{k=1}^\infty$  is nonincreasing. Since  $F_\beta(V^k, W^k) \geq 0$  for all  $k \in \mathbb{N}$ , its limit  $\lim_{k \rightarrow \infty} F_\beta(V^k, W^k)$  exists. From (22)-(24), we have

$$F_\beta(V^+, W^+) \leq F_\beta(V^k, W^+) \leq F_\beta(V^k, W^k).$$

Taking the limit gives us

$$\lim_{k \rightarrow \infty} F_\beta(V^k, W^+) = \lim_{k \rightarrow \infty} F_\beta(V^k, W^k). \tag{26}$$

Since  $(V^*, W^*)$  is an accumulation point of  $\{(V^k, W^k)\}_{k=1}^\infty$ , there exists a subsequence  $K$  such that

$$\lim_{k \in K \rightarrow \infty} (V^k, W^k) = (V^*, W^*). \tag{27}$$

Because  $r(\cdot)$  is lower semicontinuous and  $\lim_{k \in K \rightarrow \infty} V^k = V^*$ , there exists  $k' \in K$  such that  $k \geq k'$  implies  $r(V_l^k) \geq r(V_l^*)$  for each  $l = 1, \dots, L$ . Using this result along with (23), we obtain

$$\begin{aligned} F_\beta(V, W^k) &\geq F_\beta(V^k, W^k) \\ &= \tilde{\mathcal{L}}(W^k) + \sum_{l=1}^L \left[ \lambda \left( \mathcal{R}_{GL}(W_l^k) + r(V_l^k) \right) + \frac{\beta}{2} \|V_l^k - W_l^k\|_2^2 \right] \\ &\geq \tilde{\mathcal{L}}(W^k) + \sum_{l=1}^L \left[ \lambda \left( \mathcal{R}_{GL}(W_l^k) + r(V_l^*) \right) + \frac{\beta}{2} \|V_l^k - W_l^k\|_2^2 \right] \end{aligned}$$

for  $k \geq k'$ . As  $k \in K \rightarrow \infty$ , we have

$$F_\beta(V, W^*) \geq \tilde{\mathcal{L}}(W^*) + \sum_{l=1}^L \left[ \lambda \left( \mathcal{R}_{GL}(W_l^*) + r(V_l^*) \right) + \frac{\beta}{2} \|V_l^* - W_l^*\|_2^2 \right] = F_\beta(V^*, W^*) \quad (28)$$

338 by continuity, so it follows that  $V^* \in \arg \min_V F_\beta(V, W^*)$ .

For notational convenience, let

$$\tilde{\mathcal{R}}_{\lambda, \beta}(V, W) := \sum_{l=1}^L \left[ \lambda \mathcal{R}_{GL}(W_l) + \frac{\beta}{2} \|V_l - W_l\|_2^2 \right]. \quad (29)$$

By (22), we have

$$\begin{aligned} \tilde{\mathcal{L}}(W) + \tilde{\mathcal{R}}_{\lambda, \beta}(V^k, W) &= F_\beta(V^k, W) - \lambda \sum_{i=1}^L r(V_i^k) \\ &\geq F_\beta(V^k, W^+) - \lambda \sum_{i=1}^L r(V_i^k) = \tilde{\mathcal{L}}(W^+) + \tilde{\mathcal{R}}_{\lambda, \beta}(V^k, W^+). \end{aligned} \quad (30)$$

Because  $\lim_{k \in K \rightarrow \infty} V^k$  exists, the sequence  $\{V^k\}_{k \in K}$  is bounded. If  $r(\cdot)$  is  $\ell_0$ , transformed  $\ell_1$ , or SCAD, then  $\{r(V^k)\}_{k \in K}$  is bounded. If  $r(\cdot)$  is  $\ell_1$ , then  $r(\cdot)$  is coercive. If  $r(\cdot)$  is  $\ell_1 - \alpha \ell_2$ , then  $r(\cdot)$  is bounded above by  $\ell_1$ . Overall, this follows that  $\{r(V^k)\}_{k \in K}$  bounded as well. Hence, there exists a further subsequence



$\bar{K} \subset K$  such that  $\lim_{k \in \bar{K} \rightarrow \infty} r(V^k)$  exists. So, we obtain

$$\begin{aligned}
 \lim_{k \in \bar{K} \rightarrow \infty} \tilde{\mathcal{L}}(W^+) + \tilde{\mathcal{R}}_{\lambda, \beta}(V^k, W^+) &= \lim_{k \in \bar{K} \rightarrow \infty} F_{\beta}(V^k, W^+) - \lambda \sum_{i=1}^L r(V_i^k) \\
 &= \lim_{k \in \bar{K} \rightarrow \infty} F_{\beta}(V^k, W^+) - \lim_{k \in \bar{K} \rightarrow \infty} \lambda \sum_{i=1}^L r(V_i^k) \\
 &= \lim_{k \in \bar{K} \rightarrow \infty} F_{\beta}(V^k, W^k) - \lim_{k \in \bar{K} \rightarrow \infty} \lambda \sum_{i=1}^L r(V_i^k) \tag{31} \\
 &= \lim_{k \in \bar{K} \rightarrow \infty} F_{\beta}(V^k, W^k) - \lambda \sum_{i=1}^L r(V_i^k) \\
 &= \lim_{k \in \bar{K} \rightarrow \infty} \tilde{\mathcal{L}}(W^k) + \tilde{\mathcal{R}}_{\lambda, \beta}(V^k, W^k) \\
 &= \tilde{\mathcal{L}}(W^*) + \tilde{\mathcal{R}}_{\lambda, \beta}(W^*, V^*)
 \end{aligned}$$

339 after applying (26) in the third inequality and by continuity in the last equality.

Taking the limit over the subsequence  $\bar{K}$  in (30) and applying (31), we obtain

$$\tilde{\mathcal{L}}(W) + \tilde{\mathcal{R}}_{\lambda, \beta}(V^*, W) \geq \tilde{\mathcal{L}}(W^*) + \tilde{\mathcal{R}}_{\lambda, \beta}(W^*, V^*) \tag{32}$$

by continuity. Adding  $\sum_{l=1}^L r(V_l^*)$  on both sides yields

$$F_{\beta}(V^*, W) \geq F_{\beta}(V^*, W^*), \tag{33}$$

340 which follows that  $W^* \in \arg \min_W F_{\beta}(V^*, W)$ . This completes the proof.

341 **5.2 Proof of Theorem 3**

Because  $(V^*, W^*)$  is an accumulation point, there exists a subsequence  $K$  such that  $\lim_{k \in K \rightarrow \infty} (V^k, W^k) = (V^*, W^*)$ . If  $\{F_{\beta_k}(V^k, W^k)\}_{k=1}^{\infty}$  is uniformly bounded, there exists  $M$  such that  $F_{\beta_k}(V^k, W^k) \leq M$  for all  $k \in \mathbb{N}$ . Then we have

$$M \geq F_{\beta_k}(V^k, W^k) = \tilde{\mathcal{L}}(W) + \sum_{l=1}^L \left[ \lambda \mathcal{R}_{GL}(W_l) + \lambda r(V_l) + \frac{\beta_k}{2} \|V_l - W_l\|_2^2 \right] \geq \frac{\beta_k}{2} \sum_{l=1}^L \|V_l - W_l\|_2^2$$

As a result,

$$\sum_{l=1}^L \|V_l^k - W_l^k\|_2^2 \leq \frac{2}{\beta_k} M. \tag{34}$$

Taking the limit over  $k \in K$ , we have

$$\sum_{l=1}^L \|V_l^* - W_l^*\|_2^2 = 0,$$

342 which follows that  $V^* = W^*$ . As a result,  $(V^*, W^*)$  is a feasible solution to (15).

## PERMISSION TO REUSE AND COPYRIGHT

343 Figures, tables, and images will be published under a Creative Commons CC-BY licence and  
344 permission must be obtained for use of copyrighted material from other sources (including re-  
345 published/adapted/modified/partial figures and images from the internet). It is the responsibility of the  
346 authors to acquire the licenses, to follow any citation instructions requested by third-party rights holders,  
347 and cover any supplementary charges.

## CONFLICT OF INTEREST STATEMENT

348 The authors declare that the research was conducted in the absence of any commercial or financial  
349 relationships that could be construed as a potential conflict of interest.

## AUTHOR CONTRIBUTIONS

350 KB and FP performed the experiments and analysis. All authors contributed to the design, evaluation,  
351 discussions and production of the manuscript.

## FUNDING

352 The work was partially supported by NSF grants IIS-1632935, DMS-1854434, DMS-1924548 and the  
353 Qualcomm Faculty Award.

## ACKNOWLEDGMENTS

354 The authors would like to thank Dr. Thu Dinh for helpful conversations. They also thank Christos Louizos  
355 for answering our questions we had regarding his work in [54]. Lastly, the authors thank AWS Cloud  
356 Credits for Research and Google Cloud Platform (GCP) for providing cloud based computational resources  
357 for this work.

## DATA AVAILABILITY STATEMENT

358 The datasets MNIST and CIFAR 10/100 for this study are available through the Pytorch package in  
359 Python. Codes for the numerical experiments in Section 3 are available at [https://github.com/  
360 kbui1993/Official\\_Nonconvex\\_SGL](https://github.com/kbui1993/Official_Nonconvex_SGL).

## REFERENCES

- 361 [1] Aghasi, A., Abdi, A., Nguyen, N., and Romberg, J. (2017). Net-trim: Convex pruning of deep  
362 neural networks with performance guarantee. In *Advances in Neural Information Processing Systems*.  
363 3177–3186
- 364 [2] Aghasi, A., Abdi, A., and Romberg, J. (2020). Fast convex pruning of deep neural networks. *SIAM*  
365 *Journal on Mathematics of Data Science* 2, 158–188
- 366 [3] Ahn, M., Pang, J.-S., and Xin, J. (2017). Difference-of-convex learning: directional stationarity,  
367 optimality, and sparsity. *SIAM Journal on Optimization* 27, 1637–1665
- 368 [4] Alvarez, J. M. and Salzmann, M. (2016). Learning the number of neurons in deep networks. In  
369 *Advances in Neural Information Processing Systems*. 2270–2278
- 370 [5] Antoniadis, A. and Fan, J. (2001). Regularization of wavelet approximations. *Journal of the*  
371 *American Statistical Association* 96, 939–967

- 372 [6] Ba, J. and Caruana, R. (2014). Do deep nets really need to be deep? In *Advances in Neural*  
373 *Information Processing Systems*. 2654–2662
- 374 [7] Bach, F. R. (2008). Consistency of the group lasso and multiple kernel learning. *Journal of Machine*  
375 *Learning Research* 9, 1179–1225
- 376 [8] Bao, C., Dong, B., Hou, L., Shen, Z., Zhang, X., and Zhang, X. (2016). Image restoration by  
377 minimizing zero norm of wavelet frame coefficients. *Inverse Problems* 32, 115004
- 378 [9] Breheny, P. and Huang, J. (2011). Coordinate descent algorithms for nonconvex penalized regression,  
379 with applications to biological feature selection. *The Annals of Applied Statistics* 5, 232
- 380 [10] Candès, E. J., Li, X., Ma, Y., and Wright, J. (2011). Robust principal component analysis? *Journal*  
381 *of the ACM (JACM)* 58, 1–37
- 382 [11] Candès, E. J., Romberg, J. K., and Tao, T. (2006). Stable signal recovery from incomplete and  
383 inaccurate measurements. *Communications on Pure and Applied Mathematics* 59, 1207–1223
- 384 [12] Chan, R. H., Chan, T. F., Shen, L., and Shen, Z. (2003). Wavelet algorithms for high-resolution  
385 image reconstruction. *SIAM Journal on Scientific Computing* 24, 1408–1432
- 386 [13] Chen, L.-C., Papandreou, G., Kokkinos, I., Murphy, K., and Yuille, A. L. (2017). Deeplab: Semantic  
387 image segmentation with deep convolutional nets, atrous convolution, and fully connected crfs. *IEEE*  
388 *Transactions on Pattern Analysis and Machine Intelligence* 40, 834–848
- 389 [14] Cheng, Y., Wang, D., Zhou, P., and Zhang, T. (2017). A survey of model compression and  
390 acceleration for deep neural networks. *arXiv preprint arXiv:1710.09282*
- 391 [15] Cheng, Y., Wang, D., Zhou, P., and Zhang, T. (2018). Model compression and acceleration for deep  
392 neural networks: The principles, progress, and challenges. *IEEE Signal Processing Magazine* 35,  
393 126–136
- 394 [16] Cohen, A., Dahmen, W., and DeVore, R. (2009). Compressed sensing and best  $k$ -term approximation.  
395 *Journal of the American mathematical society* 22, 211–231
- 396 [17] Denton, E. L., Zaremba, W., Bruna, J., LeCun, Y., and Fergus, R. (2014). Exploiting linear structure  
397 within convolutional networks for efficient evaluation. In *Advances in Neural Information Processing*  
398 *Systems*. 1269–1277
- 399 [18] Dinh, T. and Xin, J. (September 3-4, 2020). Convergence of a relaxed variable splitting method  
400 for learning sparse neural networks via  $\ell_1, \ell_0$ , and transformed- $\ell_1$  penalties. *arXiv preprint*  
401 *arXiv:1812.05719*, in *Proceedings of Intelligent Systems Conference (IntelliSys)*, Amsterdam, The  
402 Netherlands
- 403 [19] Dong, B. and Zhang, Y. (2013). An efficient algorithm for  $\ell_0$  minimization in wavelet frame based  
404 image restoration. *Journal of Scientific Computing* 54, 350–368
- 405 [20] Donoho, D. L. and Elad, M. (2003). Optimally sparse representation in general (nonorthogonal)  
406 dictionaries via  $\ell_1$  minimization. *Proceedings of the National Academy of Sciences* 100, 2197–2202
- 407 [21] Esser, E., Lou, Y., and Xin, J. (2013). A method for finding structured sparse solutions to nonnegative  
408 least squares problems with applications. *SIAM Journal on Imaging Sciences* 6, 2010–2046
- 409 [22] Fan, J. and Li, R. (2001). Variable selection via nonconcave penalized likelihood and its oracle  
410 properties. *Journal of the American statistical Association* 96, 1348–1360
- 411 [23] Foucart, S. and Rauhut, H. (2013). An invitation to compressive sensing. In *A mathematical*  
412 *introduction to compressive sensing* (Springer). 1–39
- 413 [24] Gupta, R. and Roughgarden, T. (2017). A pac approach to application-specific algorithm selection.  
414 *SIAM Journal on Computing* 46, 992–1017
- 415 [25] Han, S., Mao, H., and Dally, W. J. (2015). Deep compression: Compressing deep neural networks  
416 with pruning, trained quantization and huffman coding. *arXiv preprint arXiv:1510.00149*

- 417 [26] Han, S., Pool, J., Tran, J., and Dally, W. (2015). Learning both weights and connections for efficient  
418 neural network. In *Advances in Neural Information Processing Systems*. 1135–1143
- 419 [27] Hastie, T., Tibshirani, R., and Friedman, J. (2009). *The elements of statistical learning: data mining,*  
420 *inference, and prediction* (Springer Science & Business Media)
- 421 [28] He, K., Zhang, X., Ren, S., and Sun, J. (2016). Deep residual learning for image recognition. In  
422 *Proceedings of the IEEE conference on computer vision and pattern recognition*. 770–778
- 423 [29] Hu, H., Peng, R., Tai, Y.-W., and Tang, C.-K. (2016). Network trimming: A data-driven neuron  
424 pruning approach towards efficient deep architectures. *arXiv preprint arXiv:1607.03250*
- 425 [30] Huang, J., Rathod, V., Sun, C., Zhu, M., Korattikara, A., Fathi, A., et al. (2017). Speed/accuracy  
426 trade-offs for modern convolutional object detectors. In *Proceedings of the IEEE conference on*  
427 *computer vision and pattern recognition*. 7310–7311
- 428 [31] Jia, Y., Shelhamer, E., Donahue, J., Karayev, S., Long, J., Girshick, R., et al. (2014). Caffe:  
429 Convolutional architecture for fast feature embedding. In *Proceedings of the 22nd ACM international*  
430 *conference on Multimedia* (ACM), 675–678
- 431 [32] Jin, X., Yuan, X., Feng, J., and Yan, S. (2016). Training skinny deep neural networks with iterative  
432 hard thresholding methods. *arXiv preprint arXiv:1607.05423*
- 433 [33] Jung, H., Ye, J. C., and Kim, E. Y. (2007). Improved k–t blast and k–t sense using focuss. *Physics in*  
434 *Medicine & Biology* 52, 3201
- 435 [34] Jung, M. (2017). Piecewise-smooth image segmentation models with  $L^1$  data-fidelity terms. *Journal*  
436 *of Scientific Computing* 70, 1229–1261
- 437 [35] Jung, M., Kang, M., and Kang, M. (2014). Variational image segmentation models involving  
438 non-smooth data-fidelity terms. *Journal of scientific computing* 59, 277–308
- 439 [36] Kim, C. and Klabjan, D. (2019). A simple and fast algorithm for L1-norm kernel pca. *IEEE*  
440 *transactions on pattern analysis and machine intelligence*
- 441 [37] Kingma, D. P. and Ba, J. (2014). Adam: A method for stochastic optimization. *arXiv preprint*  
442 *arXiv:1412.6980*
- 443 [38] Krizhevsky, A. and Hinton, G. (2009). *Learning multiple layers of features from tiny images*. Tech.  
444 rep., Citeseer
- 445 [39] Krizhevsky, A., Sutskever, I., and Hinton, G. E. (2012). Imagenet classification with deep  
446 convolutional neural networks. In *Advances in neural information processing systems*. 1097–1105
- 447 [40] Krogh, A. and Hertz, J. A. (1992). A simple weight decay can improve generalization. In *Advances*  
448 *in neural information processing systems*. 950–957
- 449 [41] LeCun, Y., Bottou, L., Bengio, Y., Haffner, P., et al. (1998). Gradient-based learning applied to  
450 document recognition. *Proceedings of the IEEE* 86, 2278–2324
- 451 [42] Li, F., Osher, S., Qin, J., and Yan, M. (2016). A multiphase image segmentation based on fuzzy  
452 membership functions and l1-norm fidelity. *Journal of Scientific Computing* 69, 82–106
- 453 [43] Li, H., Kadav, A., Durdanovic, I., Samet, H., and Graf, H. P. (2016). Pruning filters for efficient  
454 convnets. *arXiv preprint arXiv:1608.08710*
- 455 [44] Li, P., Chen, W., Ge, H., and Ng, M. K. (2020).  $\ell_1 - \alpha\ell_2$  minimization methods for signal and image  
456 reconstruction with impulsive noise removal. *Inverse Problems* 36, 055009
- 457 [45] Li, Z., Luo, X., Wang, B., Bertozzi, A. L., and Xin, J. (2019). A study on graph-structured recurrent  
458 neural networks and sparsification with application to epidemic forecasting. In *World Congress on*  
459 *Global Optimization* (Springer), 730–739
- 460 [46] Lim, M., Ales, J. M., Cottureau, B. R., Hastie, T., and Norcia, A. M. (2017). Sparse EEG/MEG  
461 source estimation via a group lasso. *PloS one* 12, e0176835

- 462 [47] Lin, D., Calhoun, V. D., and Wang, Y.-P. (2014). Correspondence between fMRI and SNP data by  
463 group sparse canonical correlation analysis. *Medical image analysis* 18, 891–902
- 464 [48] Lin, D., Zhang, J., Li, J., Calhoun, V. D., Deng, H.-W., and Wang, Y.-P. (2013). Group sparse  
465 canonical correlation analysis for genomic data integration. *BMC bioinformatics* 14, 1–16
- 466 [49] Long, J., Shelhamer, E., and Darrell, T. (2015). Fully convolutional networks for semantic  
467 segmentation. In *Proceedings of the IEEE conference on computer vision and pattern recognition*.  
468 3431–3440
- 469 [50] Lou, Y., Osher, S., and Xin, J. (2015). Computational aspects of constrained  $L_1 - L_2$  minimization  
470 for compressive sensing. In *Modelling, Computation and Optimization in Information Systems and*  
471 *Management Sciences* (Springer). 169–180
- 472 [51] Lou, Y. and Yan, M. (2018). Fast  $L_1 - L_2$  minimization via a proximal operator. *Journal of Scientific*  
473 *Computing* 74, 767–785
- 474 [52] Lou, Y., Yin, P., He, Q., and Xin, J. (2015). Computing sparse representation in a highly coherent  
475 dictionary based on difference of  $L_1$  and  $L_2$ . *Journal of Scientific Computing* 64, 178–196
- 476 [53] Lou, Y., Zeng, T., Osher, S., and Xin, J. (2015). A weighted difference of anisotropic and isotropic  
477 total variation model for image processing. *SIAM Journal on Imaging Sciences* 8, 1798–1823
- 478 [54] Louizos, C., Welling, M., and Kingma, D. P. (2017). Learning sparse neural networks through  $l_0$   
479 regularization. *International Conference on Learning Representations, 2018; CoRR* abs/1712.01312
- 480 [55] Lu, J., Qiao, K., Li, X., Lu, Z., and Zou, Y. (2019).  $l_0$ -minimization methods for image restoration  
481 problems based on wavelet frames. *Inverse Problems* 35, 064001
- 482 [56] Lu, Z. and Zhang, Y. (2013). Sparse approximation via penalty decomposition methods. *SIAM*  
483 *Journal on Optimization* 23, 2448–2478
- 484 [57] Lustig, M., Donoho, D., and Pauly, J. M. (2007). Sparse mri: The application of compressed sensing  
485 for rapid mr imaging. *Magnetic Resonance in Medicine: An Official Journal of the International*  
486 *Society for Magnetic Resonance in Medicine* 58, 1182–1195
- 487 [58] Lv, J., Fan, Y., et al. (2009). A unified approach to model selection and sparse recovery using  
488 regularized least squares. *The Annals of Statistics* 37, 3498–3528
- 489 [59] Lyu, J., Zhang, S., Qi, Y., and Xin, J. (2020). Autosshufflenet: Learning permutation matrices via an  
490 exact Lipschitz continuous penalty in deep convolutional neural networks. In *Proceedings of the*  
491 *26th ACM SIGKDD International Conference on Knowledge Discovery & Data Mining*. 608–616
- 492 [60] Ma, N., Zhang, X., Zheng, H.-T., and Sun, J. (2018). Shufflenet v2: Practical guidelines for efficient  
493 cnn architecture design. In *Proceedings of the European conference on computer vision (ECCV)*.  
494 116–131
- 495 [61] Ma, R., Miao, J., Niu, L., and Zhang, P. (2019). Transformed  $l_1$  regularization for learning sparse  
496 deep neural networks. *arXiv preprint arXiv:1901.01021*
- 497 [62] Ma, S., Song, X., and Huang, J. (2007). Supervised group lasso with applications to microarray data  
498 analysis. *BMC bioinformatics* 8, 60
- 499 [63] Ma, T.-H., Lou, Y., Huang, T.-Z., and Zhao, X.-L. (2017). Group-based truncated  $L_{1-2}$  model  
500 for image inpainting. In *2017 IEEE International Conference on Image Processing (ICIP) (IEEE)*,  
501 2079–2083
- 502 [64] Mehranian, A., Rad, H. S., Rahmim, A., Ay, M. R., and Zaidi, H. (2013). Smoothly Clipped Absolute  
503 Deviation (SCAD) regularization for compressed sensing MRI using an augmented lagrangian  
504 scheme. *Magnetic resonance imaging* 31, 1399–1411
- 505 [65] Meier, L., Van De Geer, S., and Bühlmann, P. (2008). The group lasso for logistic regression. *Journal*  
506 *of the Royal Statistical Society: Series B (Statistical Methodology)* 70, 53–71

- 507 [66] Molchanov, D., Ashukha, A., and Vetrov, D. (2017). Variational dropout sparsifies deep neural  
508 networks. In *Proceedings of the 34th International Conference on Machine Learning-Volume 70*  
509 (JMLR. org), 2498–2507
- 510 [67] Nie, F., Wang, H., Huang, H., and Ding, C. (2011). Unsupervised and semi-supervised learning via  
511  $\ell_1$ -norm graph. In *2011 International Conference on Computer Vision (IEEE)*, 2268–2273
- 512 [68] Nikolova, M. (2000). Local strong homogeneity of a regularized estimator. *SIAM Journal on Applied*  
513 *Mathematics* 61, 633–658
- 514 [69] Nocedal, J. and Wright, S. (2006). *Numerical optimization* (Springer Science & Business Media)
- 515 [70] Parikh, N., Boyd, S., et al. (2014). Proximal algorithms. *Foundations and Trends® in Optimization*  
516 1, 127–239
- 517 [71] Park, F., Lou, Y., and Xin, J. (2016). A weighted difference of anisotropic and isotropic total variation  
518 for relaxed mumford-shah image segmentation. In *2016 IEEE International Conference on Image*  
519 *Processing (ICIP) (IEEE)*, 4314–4318
- 520 [72] Parkhi, O. M., Vedaldi, A., Zisserman, A., et al. (2015). Deep face recognition. In *bmvc*. 6
- 521 [73] Ren, S., He, K., Girshick, R., and Sun, J. (2015). Faster r-cnn: Towards real-time object detection  
522 with region proposal networks. In *Advances in neural information processing systems*. 91–99
- 523 [74] Santosa, F. and Symes, W. W. (1986). Linear inversion of band-limited reflection seismograms.  
524 *SIAM Journal on Scientific and Statistical Computing* 7, 1307–1330
- 525 [75] Scardapane, S., Comminiello, D., Hussain, A., and Uncini, A. (2017). Group sparse regularization  
526 for deep neural networks. *Neurocomputing* 241, 81–89
- 527 [76] Simon, N., Friedman, J., Hastie, T., and Tibshirani, R. (2013). A sparse-group lasso. *Journal of*  
528 *Computational and Graphical Statistics* 22, 231–245
- 529 [77] Simonyan, K. and Zisserman, A. (2015). Very deep convolutional networks for large-scale image  
530 recognition. *CoRR* abs/1409.1556
- 531 [78] Tibshirani, R. (1996). Regression shrinkage and selection via the lasso. *Journal of the Royal*  
532 *Statistical Society: Series B (Methodological)* 58, 267–288
- 533 [79] Tran, H. and Webster, C. (2019). A class of null space conditions for sparse recovery via nonconvex,  
534 non-separable minimizations. *Results in Applied Mathematics* 3, 100011
- 535 [80] Trzasko, J., Manduca, A., and Borisch, E. (2007). Sparse mri reconstruction via multiscale  $L_0$ -  
536 continuation. In *2007 IEEE/SP 14th Workshop on Statistical Signal Processing (IEEE)*, 176–180
- 537 [81] Ullrich, K., Meeds, E., and Welling, M. (2017). Soft weight-sharing for neural network compression.  
538 *stat* 1050, 9
- 539 [82] Vershynin, R. (2018). *High-dimensional probability: An introduction with applications in data*  
540 *science*, vol. 47 (Cambridge university press)
- 541 [83] Vincent, M. and Hansen, N. R. (2014). Sparse group lasso and high dimensional multinomial  
542 classification. *Computational Statistics & Data Analysis* 71, 771–786
- 543 [84] Wang, L., Chen, G., and Li, H. (2007). Group scad regression analysis for microarray time course  
544 gene expression data. *Bioinformatics* 23, 1486–1494
- 545 [85] Wen, F., Chu, L., Liu, P., and Qiu, R. C. (2018). A survey on nonconvex regularization-based  
546 sparse and low-rank recovery in signal processing, statistics, and machine learning. *IEEE Access* 6,  
547 69883–69906
- 548 [86] Wen, W., Wu, C., Wang, Y., Chen, Y., and Li, H. (2016). Learning structured sparsity in deep neural  
549 networks. In *Advances in neural information processing systems*. 2074–2082
- 550 [87] Xue, F. and Xin, J. (2019). Learning sparse neural networks via  $\ell_0$  and  $T\ell_1$  by a relaxed variable  
551 splitting method with application to multi-scale curve classification. In *World Congress on Global*

- 552 Optimization (Springer), 800–809
- 553 [88] Yang, C., Akimoto, Y., Kim, D. W., and Udell, M. (2019). Oboe: Collaborative filtering for automl  
554 model selection. In *Proceedings of the 25th ACM SIGKDD International Conference on Knowledge  
555 Discovery & Data Mining*. 1173–1183
- 556 [89] Ye, Q., Zhao, H., Li, Z., Yang, X., Gao, S., Yin, T., et al. (2017). L1-norm distance minimization-  
557 based fast robust twin support vector  $k$ -plane clustering. *IEEE transactions on neural networks and  
558 learning systems* 29, 4494–4503
- 559 [90] Yin, P., Lou, Y., He, Q., and Xin, J. (2015). Minimization of  $\ell_{1-2}$  for compressed sensing. *SIAM  
560 Journal on Scientific Computing* 37, A536–A563
- 561 [91] Yin, P., Sun, Z., Jin, W.-L., and Xin, J. (2017).  $\ell_1$ -minimization method for link flow correction.  
562 *Transportation Research Part B: Methodological* 104, 398–408
- 563 [92] Yoon, J. and Hwang, S. J. (2017). Combined group and exclusive sparsity for deep neural networks.  
564 In *Proceedings of the 34th International Conference on Machine Learning-Volume 70* (JMLR. org),  
565 3958–3966
- 566 [93] Yuan, M. and Lin, Y. (2006). Model selection and estimation in regression with grouped variables.  
567 *Journal of the Royal Statistical Society: Series B (Statistical Methodology)* 68, 49–67
- 568 [94] Yuan, X.-T., Li, P., and Zhang, T. (2017). Gradient hard thresholding pursuit. *Journal of Machine  
569 Learning Research* 18, 166–1
- 570 [95] Zagoruyko, S. and Komodakis, N. (2016). Wide residual networks. *arXiv preprint arXiv:1605.07146*
- 571 [96] Zhang, C., Bengio, S., Hardt, M., Recht, B., and Vinyals, O. (2016). Understanding deep learning  
572 requires rethinking generalization. *arXiv preprint arXiv:1611.03530*
- 573 [97] Zhang, S. and Xin, J. (2017). Minimization of transformed  $l_1$  penalty: Closed form representation  
574 and iterative thresholding algorithms. *Communications in Mathematical Sciences* 15, 511 – 537
- 575 [98] Zhang, S. and Xin, J. (2018). Minimization of transformed  $l_1$  penalty: theory, difference of convex  
576 function algorithm, and robust application in compressed sensing. *Mathematical Programming* 169,  
577 307–336
- 578 [99] Zhang, S., Yin, P., and Xin, J. (2017). Transformed Schatten-1 iterative thresholding algorithms for  
579 low rank matrix completion. *Communications in Mathematical Sciences* 15, 839 – 862
- 580 [100] Zhang, X., Lu, Y., and Chan, T. (2012). A novel sparsity reconstruction method from poisson data  
581 for 3d bioluminescence tomography. *Journal of scientific computing* 50, 519–535
- 582 [101] Zhang, X., Zhou, X., Lin, M., and Sun, J. (2018). Shufflenet: An extremely efficient convolutional  
583 neural network for mobile devices. In *Proceedings of the IEEE conference on computer vision and  
584 pattern recognition*. 6848–6856
- 585 [102] Zhang, Y., Dong, B., and Lu, Z. (2013).  $\ell_0$  minimization for wavelet frame based image restoration.  
586 *Mathematics of Computation* 82, 995–1015
- 587 [103] Zhou, H., Sehl, M. E., Sinsheimer, J. S., and Lange, K. (2010). Association screening of common  
588 and rare genetic variants by penalized regression. *Bioinformatics* 26, 2375
- 589 [104] Zhou, Y., Jin, R., and Hoi, S. C.-H. (2010). Exclusive lasso for multi-task feature selection. In  
590 *Proceedings of the Thirteenth International Conference on Artificial Intelligence and Statistics*.  
591 988–995
- 592 [105] Zhuang, Z., Tan, M., Zhuang, B., Liu, J., Guo, Y., Wu, Q., et al. (2018). Discrimination-aware  
593 channel pruning for deep neural networks. In *Advances in Neural Information Processing Systems*.  
594 875–886

**Table 1.** Regularization penalties and their corresponding proximal operators with  $\lambda > 0$ .

Regularizer Name	Penalty Formulation	Proximal Operator
$\ell_1$	$\lambda \ x\ _1 = \lambda \sum_{i=1}^n  x_i $	$\text{prox}_{\lambda \ \cdot\ _1}(x) = (\mathcal{S}_\lambda(x_1), \dots, \mathcal{S}_\lambda(x_n)),$ <p>with</p> $\mathcal{S}_\lambda(t) = \text{sign}(t) \max\{ t  - \lambda, 0\}$
$\ell_0$	$\lambda \ x\ _0 = \lambda \sum_{i=1}^n  x_i _0$	$\text{prox}_{\lambda \ \cdot\ _0}(x) = (\mathcal{H}_\lambda(x_1), \dots, \mathcal{H}_\lambda(x_n)),$ <p>with</p> $\mathcal{H}_\lambda(t) = \begin{cases} 0 & \text{if }  t  \leq \sqrt{2\lambda} \\ t & \text{if }  t  > \sqrt{2\lambda} \end{cases}$
SCAD(a)	$\lambda \ x\ _{\text{SCAD}(a)} = \sum_{i=1}^n \lambda  x_i _{\text{SCAD}(a)}$ <p>with</p> $\lambda  t _{\text{SCAD}(a)} = \begin{cases} \lambda  t  & \text{if }  t  < \lambda \\ \frac{2a\lambda t  - t^2 - \lambda^2}{2(a-1)} & \text{if } \lambda \leq  t  < a\lambda \\ (a+1)\lambda^2/2 & \text{if }  t  \geq a\lambda \end{cases}$	$\text{prox}_{\lambda \ \cdot\ _{\text{SCAD}(a)}}(x) = (\mathcal{S}_{a,\lambda}(x_1), \dots, \mathcal{S}_{a,\lambda}(x_n)),$ <p>with</p> $\mathcal{S}_{a,\lambda}(t) = \begin{cases} \mathcal{S}_\lambda(t) & \text{if }  t  \leq 2\lambda \\ \frac{(a-1)t - \text{sign}(t)a\lambda}{a-2} & \text{if } 2\lambda <  t  \leq a\lambda \\ t & \text{if }  t  > a\lambda. \end{cases}$
TL1(a)	$\lambda \ x\ _{\text{TL1}(a)} = \lambda \sum_{i=1}^n \frac{(a+1) x_i }{a +  x_i }$	$\text{prox}_{\lambda \ \cdot\ _{\text{TL1}(a)}}(x) = (\mathcal{T}_{a,\lambda}(x_1), \dots, \mathcal{T}_{a,\lambda}(x_n)),$ <p>with</p> $\mathcal{T}_{a,\lambda}(t) = \begin{cases} 0 & \text{if }  t  \leq \tau(a, \lambda) \\ g_{a,\lambda}(t) & \text{if }  t  > \tau(a, \lambda) \end{cases}$ <p>where</p> $g_{a,\lambda}(t) = \text{sign}(t) \left( \frac{2}{3}(a +  t ) \cos\left(\frac{\phi_{a,\lambda}(t)}{3}\right) - \frac{2a}{3} + \frac{ t }{3} \right),$ $\phi_{a,\lambda}(t) = \arccos\left(1 - \frac{27\lambda a(a+1)}{2(a+ t )^3}\right),$ <p>and</p> $\tau(a, \lambda) = \begin{cases} \sqrt{2\lambda(a+1)} - \frac{a}{2} & \text{if } \lambda > \frac{a^2}{2(a+1)} \\ \lambda \frac{a+1}{a} & \text{if } \lambda \leq \frac{a^2}{2(a+1)} \end{cases}$
$\ell_1 - \ell_2$	$\lambda \ x\ _{\ell_1 - \ell_2} = \lambda \left( \sum_{i=1}^n  x_i  - \sqrt{\sum_{i=1}^n x_i^2} \right)$	$\text{prox}_{\lambda \ \cdot\ _{\ell_1 - \ell_2}}(x) = \begin{cases} \frac{\ z_1\ _2 + \lambda}{\ z_1\ _2} z_1 & \text{if } \ x\ _\infty > \lambda \\ z_2 & \text{if } 0 \leq \ x\ _\infty \leq \lambda \end{cases}$ <p>with <math>z_1 = \mathcal{S}_\lambda(x)</math> and</p> $(z_2)_i = \begin{cases} 0 & \text{if } i \neq k \\ \text{sign}(x_i) \ x\ _\infty & \text{if } i = k, \end{cases}$ <p>where <math>k = \arg \min_{1 \leq k \leq n} \{  x_k  = \ x\ _\infty \}</math>.</p>



**Table 2.** Average test error, weight sparsity, and neuron sparsity of Lenet-5 models trained on MNIST after 200 epochs across 5 runs. Standard deviations are in parentheses.

Avg. Test Error (%)	$\ell_0$	CGES	GL	SGL <sub>1</sub>	SGL <sub>0</sub>	SGSCAD	SGTL <sub>1</sub>	SGL <sub>1</sub> - L <sub>2</sub>
$\alpha = 0.1$	0.816 (0.024)	<b>0.644</b> (0.039)	0.742 (0.030)	0.722 (0.028)	0.682 (0.044)	0.734 (0.039)	0.716 (0.048)	0.688 (0.034)
$\alpha = 0.2$	0.914 (0.029)	0.718 (0.044)	0.772 (0.031)	<b>0.704</b> (0.031)	0.712 (0.042)	0.788 (0.045)	0.718 (0.025)	0.746 (0.031)
$\alpha = 0.3$	1.032 (0.045)	<b>0.678</b> (0.007)	0.782 (0.035)	0.732 (0.045)	0.686 (0.048)	0.760 (0.037)	0.728 (0.034)	0.712 (0.061)
$\alpha = 0.4$	1.062 (0.030)	<b>0.662</b> (0.024)	0.820 (0.054)	0.792 (0.034)	0.704 (0.033)	0.786 (0.045)	0.766 (0.045)	0.756 (0.014)
$\alpha = 0.5$	1.098 (0.035)	0.696 (0.016)	0.834 (0.033)	0.720 (0.039)	<b>0.630</b> (0.024)	0.728 (0.044)	0.684 (0.024)	0.750 (0.017)
Avg. Weight Sparsity	$\ell_0$	CGES	GL	SGL <sub>1</sub>	SGL <sub>0</sub>	SGSCAD	SGTL <sub>1</sub>	SGL <sub>1</sub> - L <sub>2</sub>
$\alpha = 0.1$	$2.12 \times 10^{-4}$ ( $1.54 \times 10^{-5}$ )	<b>0.940</b> ( $1.51 \times 10^{-3}$ )	0.885 ( $2.25 \times 10^{-3}$ )	0.889 ( $4.30 \times 10^{-3}$ )	0.894 ( $3.81 \times 10^{-3}$ )	0.894 ( $3.61 \times 10^{-3}$ )	0.901 ( $1.57 \times 10^{-3}$ )	0.893 ( $2.77 \times 10^{-3}$ )
$\alpha = 0.2$	$2.16 \times 10^{-4}$ ( $3.76 \times 10^{-6}$ )	<b>0.952</b> ( $1.51 \times 10^{-3}$ )	0.922 ( $2.07 \times 10^{-3}$ )	0.926 ( $1.19 \times 10^{-3}$ )	0.926 ( $1.75 \times 10^{-3}$ )	0.926 ( $3.31 \times 10^{-3}$ )	0.930 ( $2.37 \times 10^{-3}$ )	0.923 ( $2.86 \times 10^{-3}$ )
$\alpha = 0.3$	$2.24 \times 10^{-4}$ ( $5.35 \times 10^{-6}$ )	<b>0.956</b> ( $1.41 \times 10^{-3}$ )	0.933 ( $1.03 \times 10^{-3}$ )	0.945 ( $1.43 \times 10^{-3}$ )	0.941 ( $1.73 \times 10^{-3}$ )	0.941 ( $2.52 \times 10^{-3}$ )	0.941 ( $1.28 \times 10^{-3}$ )	0.943 ( $1.04 \times 10^{-3}$ )
$\alpha = 0.4$	$2.06 \times 10^{-4}$ ( $6.27 \times 10^{-6}$ )	<b>0.960</b> ( $1.05 \times 10^{-3}$ )	0.943 ( $1.63 \times 10^{-3}$ )	0.952 ( $1.21 \times 10^{-3}$ )	0.951 ( $1.82 \times 10^{-3}$ )	0.950 ( $1.64 \times 10^{-3}$ )	0.952 ( $1.91 \times 10^{-3}$ )	0.952 ( $1.14 \times 10^{-3}$ )
$\alpha = 0.5$	$2.27 \times 10^{-4}$ ( $1.53 \times 10^{-5}$ )	<b>0.963</b> ( $1.85 \times 10^{-3}$ )	0.946 ( $1.43 \times 10^{-3}$ )	0.954 ( $1.63 \times 10^{-3}$ )	0.957 ( $9.21 \times 10^{-4}$ )	0.956 ( $1.37 \times 10^{-3}$ )	0.956 ( $2.00 \times 10^{-3}$ )	0.956 ( $2.43 \times 10^{-3}$ )
Avg. Neuron Sparsity	$\ell_0$	CGES	GL	SGL <sub>1</sub>	SGL <sub>0</sub>	SGSCAD	SGTL <sub>1</sub>	SGL <sub>1</sub> - L <sub>2</sub>
$\alpha = 0.1$	0.531 ( $3.79 \times 10^{-4}$ )	0.387 ( $9.13 \times 10^{-3}$ )	0.696 ( $2.42 \times 10^{-3}$ )	0.691 ( $7.38 \times 10^{-3}$ )	0.682 ( $6.27 \times 10^{-3}$ )	<b>0.704</b> ( $3.94 \times 10^{-3}$ )	0.703 ( $5.09 \times 10^{-3}$ )	0.697 ( $3.93 \times 10^{-3}$ )
$\alpha = 0.2$	0.578 ( $1.19 \times 10^{-3}$ )	0.449 ( $1.26 \times 10^{-2}$ )	0.756 ( $3.39 \times 10^{-3}$ )	0.754 ( $2.72 \times 10^{-3}$ )	0.740 ( $4.01 \times 10^{-3}$ )	<b>0.758</b> ( $5.78 \times 10^{-3}$ )	0.757 ( $3.93 \times 10^{-3}$ )	0.749 ( $6.50 \times 10^{-3}$ )
$\alpha = 0.3$	0.602 ( $4.42 \times 10^{-4}$ )	0.476 ( $1.17 \times 10^{-2}$ )	0.776 ( $3.18 \times 10^{-3}$ )	<b>0.787</b> ( $2.55 \times 10^{-3}$ )	0.769 ( $4.44 \times 10^{-3}$ )	0.785 ( $4.97 \times 10^{-3}$ )	0.774 ( $4.11 \times 10^{-3}$ )	0.783 ( $3.78 \times 10^{-3}$ )
$\alpha = 0.4$	0.616 ( $7.58 \times 10^{-4}$ )	0.518 ( $9.72 \times 10^{-3}$ )	0.795 ( $3.44 \times 10^{-3}$ )	<b>0.805</b> ( $3.89 \times 10^{-3}$ )	0.791 ( $5.40 \times 10^{-3}$ )	0.803 ( $3.35 \times 10^{-3}$ )	0.799 ( $3.56 \times 10^{-3}$ )	0.804 ( $2.69 \times 10^{-3}$ )
$\alpha = 0.5$	0.626 ( $1.07 \times 10^{-3}$ )	0.539 ( $1.27 \times 10^{-2}$ )	0.799 ( $2.59 \times 10^{-3}$ )	0.811 ( $4.07 \times 10^{-3}$ )	0.807 ( $3.15 \times 10^{-3}$ )	<b>0.819</b> ( $2.79 \times 10^{-3}$ )	0.811 ( $6.29 \times 10^{-3}$ )	0.815 ( $6.10 \times 10^{-3}$ )

**Table 3.** Average test error, weight sparsity, and neuron sparsity of Lenet-5 models trained on MNIST with lowest test errors across 5 runs. Standard deviations are in parentheses.

Avg. Test Error (%)	$\ell_0$	CGES	$GL$	$SGL_1$	$SGL_0$	$SGSCAD$	$SGTL_1$	$SGL_1 - L_2$
$\alpha = 0.1$	0.682 (0.023)	<b>0.532</b> (0.031)	0.568 (0.026)	0.568 (0.021)	0.576 (0.027)	0.602 (0.027)	0.582 (0.028)	0.554 (0.056)
$\alpha = 0.2$	0.846 (0.033)	0.584 (0.038)	0.630 (0.017)	0.582 (0.035)	0.584 (0.049)	0.616 (0.021)	0.592 (0.026)	<b>0.578</b> (0.032)
$\alpha = 0.3$	0.980 (0.033)	0.590 (0.028)	0.642 (0.013)	0.600 (0.030)	<b>0.588</b> (0.019)	0.618 (0.037)	0.594 (0.022)	0.596 (0.039)
$\alpha = 0.4$	1.014 (0.019)	<b>0.562</b> (0.015)	0.680 (0.038)	0.652 (0.025)	0.604 (0.033)	0.630 (0.035)	0.630 (0.048)	0.628 (0.020)
$\alpha = 0.5$	1.066 (0.024)	0.598 (0.027)	0.682 (0.043)	0.616 (0.052)	<b>0.572</b> (0.012)	0.654 (0.015)	0.586 (0.034)	0.670 (0.026)
Avg. Weight Sparsity	$\ell_0$	CGES	$GL$	$SGL_1$	$SGL_0$	$SGSCAD$	$SGTL_1$	$SGL_1 - L_2$
$\alpha = 0.1$	$2.38 \times 10^{-4}$ ( $1.97 \times 10^{-5}$ )	0.541 (0.024)	0.661 (0.073)	0.757 (0.015)	0.768 (0.019)	0.680 (0.167)	<b>0.773</b> ( $7.48 \times 10^{-3}$ )	0.719 (0.066)
$\alpha = 0.2$	$2.26 \times 10^{-4}$ ( $9.43 \times 10^{-6}$ )	0.583 (0.017)	0.728 (0.170)	0.845 ( $4.79 \times 10^{-3}$ )	<b>0.857</b> ( $6.15 \times 10^{-3}$ )	0.821 (0.041)	0.854 ( $5.60 \times 10^{-3}$ )	0.836 ( $6.76 \times 10^{-3}$ )
$\alpha = 0.3$	$2.19 \times 10^{-4}$ ( $1.36 \times 10^{-5}$ )	0.603 (0.020)	0.810 (0.078)	0.886 ( $3.69 \times 10^{-3}$ )	<b>0.889</b> ( $3.62 \times 10^{-3}$ )	0.878 ( $9.43 \times 10^{-4}$ )	0.827 (0.115)	0.879 ( $3.97 \times 10^{-3}$ )
$\alpha = 0.4$	$2.22 \times 10^{-4}$ ( $1.47 \times 10^{-5}$ )	0.627 (0.019)	0.845 (0.040)	0.896 ( $3.57 \times 10^{-3}$ )	<b>0.905</b> ( $3.66 \times 10^{-3}$ )	0.846 (0.097)	0.899 ( $4.23 \times 10^{-3}$ )	0.852 (0.097)
$\alpha = 0.5$	$2.24 \times 10^{-4}$ ( $1.02 \times 10^{-5}$ )	0.633 (0.013)	0.886 ( $6.40 \times 10^{-3}$ )	0.905 ( $2.87 \times 10^{-3}$ )	<b>0.922</b> (0.015)	0.902 ( $2.64 \times 10^{-3}$ )	0.871 (0.084)	0.848 (0.080)
Avg. Neuron Sparsity	$\ell_0$	CGES	$GL$	$SGL_1$	$SGL_0$	$SGSCAD$	$SGTL_1$	$SGL_1 - L_2$
$\alpha = 0.1$	0.363 (0.047)	0.315 (0.030)	0.389 (0.120)	0.497 (0.014)	0.496 (0.030)	0.426 (0.172)	<b>0.513</b> ( $9.57 \times 10^{-3}$ )	0.440 (0.107)
$\alpha = 0.2$	0.574 ( $2.22 \times 10^{-3}$ )	0.392 (0.016)	0.498 (0.185)	0.627 (0.011)	0.631 (0.012)	0.549 (0.169)	<b>0.634</b> ( $9.30 \times 10^{-3}$ )	0.608 (0.015)
$\alpha = 0.3$	0.599 ( $2.61 \times 10^{-3}$ )	0.418 (0.021)	0.570 (0.154)	<b>0.697</b> ( $9.73 \times 10^{-3}$ )	0.692 ( $8.19 \times 10^{-3}$ )	0.684 ( $5.69 \times 10^{-3}$ )	0.613 (0.154)	0.686 ( $8.60 \times 10^{-3}$ )
$\alpha = 0.4$	0.614 ( $1.71 \times 10^{-3}$ )	0.482 (0.020)	0.586 (0.184)	0.721 ( $8.16 \times 10^{-3}$ )	<b>0.725</b> ( $9.97 \times 10^{-3}$ )	0.642 (0.151)	0.724 (0.015)	0.655 (0.150)
$\alpha = 0.5$	0.625 ( $1.55 \times 10^{-3}$ )	0.492 (0.024)	0.708 ( $8.94 \times 10^{-3}$ )	0.735 ( $3.73 \times 10^{-3}$ )	<b>0.759</b> (0.020)	0.733 ( $8.59 \times 10^{-3}$ )	0.683 (0.143)	0.570 (0.216)

**Table 4.** Average test error, weight sparsity, and neuron sparsity of 4-layer CNN models trained on MNIST after 200 epochs across 5 runs. Standard deviations are in parentheses.

Avg. Test Error (%)	$\ell_0$	CGES	GL	$SGL_1$	$SGL_0$	SGSCAD	$SGTL_1$	$SGL_1 - L_2$
$\alpha = 0.2$	0.962 (0.041)	0.470 (0.036)	0.486 (0.030)	0.418 (0.010)	0.432 (0.023)	<b>0.408</b> (0.013)	0.418 (0.026)	0.436 (0.012)
$\alpha = 0.4$	1.454 (0.070)	0.486 (0.030)	0.502 (0.035)	<b>0.436</b> (0.026)	0.49 (0.017)	0.456 (0.016)	0.47 (0.035)	0.446 (0.031)
$\alpha = 0.6$	2.396 (0.066)	0.512 (0.035)	0.510 (0.028)	0.494 (0.031)	0.500 (0.023)	<b>0.488</b> (0.019)	0.498 (0.025)	0.522 (0.019)
$\alpha = 0.8$	3.396 (0.096)	<b>0.502</b> (0.020)	0.544 (0.026)	0.542 (0.025)	0.536 (0.037)	0.524 (0.015)	0.536 (0.014)	0.524 (0.015)
$\alpha = 1.0$	4.74 (0.148)	<b>0.524</b> (0.26)	0.568 (0.004)	0.566 (0.041)	0.576 (0.014)	0.544 (0.024)	0.552 (0.017)	0.556 (0.022)
Avg. Weight Sparsity	$\ell_0$	CGES	GL	$SGL_1$	$SGL_0$	SGSCAD	$SGTL_1$	$SGL_1 - L_2$
$\alpha = 0.2$	$5.99 \times 10^{-5}$ ( $9.28 \times 10^{-6}$ )	<b>0.655</b> ( $4.10 \times 10^{-3}$ )	0.284 ( $6.47 \times 10^{-3}$ )	0.302 ( $6.68 \times 10^{-3}$ )	0.306 (0.014)	0.297 ( $5.42 \times 10^{-3}$ )	0.298 ( $8.63 \times 10^{-3}$ )	0.299 ( $7.74 \times 10^{-3}$ )
$\alpha = 0.4$	$5.84 \times 10^{-5}$ ( $7.95 \times 10^{-6}$ )	<b>0.710</b> ( $2.45 \times 10^{-3}$ )	0.489 ( $7.38 \times 10^{-3}$ )	0.510 ( $1.85 \times 10^{-3}$ )	0.502 ( $8.01 \times 10^{-3}$ )	0.507 ( $8.80 \times 10^{-3}$ )	0.510 (0.011)	0.505 ( $7.25 \times 10^{-3}$ )
$\alpha = 0.6$	$6.06 \times 10^{-5}$ ( $1.22 \times 10^{-5}$ )	<b>0.737</b> ( $2.13 \times 10^{-3}$ )	0.593 ( $5.67 \times 10^{-3}$ )	0.606 ( $5.41 \times 10^{-3}$ )	0.603 ( $7.61 \times 10^{-3}$ )	0.605 ( $5.46 \times 10^{-3}$ )	0.599 (0.012)	0.609 ( $6.96 \times 10^{-3}$ )
$\alpha = 0.8$	$7.18 \times 10^{-5}$ ( $6.24 \times 10^{-6}$ )	<b>0.755</b> ( $5.67 \times 10^{-3}$ )	0.661 ( $6.11 \times 10^{-3}$ )	0.660 ( $6.42 \times 10^{-3}$ )	0.663 ( $7.30 \times 10^{-3}$ )	0.661 ( $8.74 \times 10^{-3}$ )	0.665 ( $3.95 \times 10^{-3}$ )	0.661 ( $5.72 \times 10^{-3}$ )
$\alpha = 1.0$	$6.90 \times 10^{-5}$ ( $7.33 \times 10^{-6}$ )	<b>0.767</b> ( $2.92 \times 10^{-3}$ )	0.695 ( $5.08 \times 10^{-3}$ )	0.696 ( $4.68 \times 10^{-3}$ )	0.697 ( $2.38 \times 10^{-4}$ )	0.698 ( $6.51 \times 10^{-3}$ )	0.699 ( $4.27 \times 10^{-3}$ )	0.689 ( $9.47 \times 10^{-3}$ )
Avg. Neuron Sparsity	$\ell_0$	CGES	GL	$SGL_1$	$SGL_0$	SGSCAD	$SGTL_1$	$SGL_1 - L_2$
$\alpha = 0.2$	<b>0.472</b> ( $7.10 \times 10^{-4}$ )	0.299 ( $2.40 \times 10^{-3}$ )	0.153 ( $4.06 \times 10^{-3}$ )	0.160 ( $4.54 \times 10^{-3}$ )	0.164 ( $8.58 \times 10^{-3}$ )	0.158 ( $3.68 \times 10^{-3}$ )	0.158 ( $5.20 \times 10^{-3}$ )	0.159 ( $5.87 \times 10^{-3}$ )
$\alpha = 0.4$	<b>0.494</b> ( $1.01 \times 10^{-3}$ )	0.329 ( $2.10 \times 10^{-3}$ )	0.280 ( $5.64 \times 10^{-3}$ )	0.287 ( $7.55 \times 10^{-4}$ )	0.280 ( $6.57 \times 10^{-3}$ )	0.281 ( $5.05 \times 10^{-3}$ )	0.285 ( $8.48 \times 10^{-3}$ )	0.284 ( $7.22 \times 10^{-3}$ )
$\alpha = 0.6$	<b>0.506</b> ( $7.23 \times 10^{-4}$ )	0.343 ( $1.78 \times 10^{-3}$ )	0.351 ( $4.72 \times 10^{-3}$ )	0.354 ( $2.47 \times 10^{-3}$ )	0.35 ( $7.17 \times 10^{-3}$ )	0.352 ( $3.99 \times 10^{-3}$ )	0.347 ( $9.65 \times 10^{-3}$ )	0.353 ( $5.88 \times 10^{-3}$ )
$\alpha = 0.8$	<b>0.516</b> ( $6.72 \times 10^{-4}$ )	0.355 ( $8.23 \times 10^{-3}$ )	0.404 ( $6.20 \times 10^{-3}$ )	0.391 ( $4.66 \times 10^{-3}$ )	0.396 ( $7.60 \times 10^{-3}$ )	0.395 ( $9.59 \times 10^{-3}$ )	0.399 ( $3.89 \times 10^{-3}$ )	0.398 ( $6.39 \times 10^{-3}$ )
$\alpha = 1.0$	<b>0.526</b> ( $9.45 \times 10^{-4}$ )	0.361 ( $5.36 \times 10^{-3}$ )	0.432 ( $5.02 \times 10^{-3}$ )	0.424 ( $5.62 \times 10^{-3}$ )	0.427 ( $2.64 \times 10^{-3}$ )	0.427 ( $7.36 \times 10^{-3}$ )	0.430 ( $6.37 \times 10^{-3}$ )	0.417 (0.011)

**Table 5.** Average test error, weight sparsity, and neuron sparsity of 4-layer CNN models trained on MNIST with lowest test errors across 5 runs. Standard deviations are in parentheses.

Avg. Test Error (%)	$\ell_0$	CGES	GL	$SGL_1$	$SGL_0$	SGSCAD	$SGTL_1$	$SGL_1 - L_2$
$\alpha = 0.2$	0.916 (0.010)	0.452 (0.033)	0.440 (0.021)	<b>0.384</b> (0.015)	0.404 (0.019)	<b>0.384</b> (0.020)	0.392 (0.023)	0.398 (0.015)
$\alpha = 0.4$	1.414 (0.073)	0.448 (0.012)	0.456 (0.024)	0.414 (0.021)	0.426 (0.016)	0.426 (0.017)	0.428 (0.034)	<b>0.412</b> (0.012)
$\alpha = 0.6$	1.890 (0.033)	0.464 (0.022)	0.472 (0.013)	<b>0.434</b> (0.010)	0.460 (0.026)	0.440 (0.017)	0.452 (0.016)	0.454 (0.024)
$\alpha = 0.8$	1.966 (0.010)	<b>0.478</b> (0.007)	0.506 (0.014)	0.484 (0.019)	0.504 (0.015)	0.482 (0.019)	0.488 (0.016)	0.492 (0.007)
$\alpha = 1.0$	2.046 (0.019)	<b>0.492</b> (0.024)	0.530 (0.014)	0.514 (0.026)	0.520 (0.035)	0.506 (0.019)	0.514 (0.014)	<b>0.492</b> (0.016)
Avg. Weight Sparsity	$\ell_0$	CGES	GL	$SGL_1$	$SGL_0$	SGSCAD	$SGTL_1$	$SGL_1 - L_2$
$\alpha = 0.2$	$5.86 \times 10^{-5}$ ( $4.32 \times 10^{-6}$ )	<b>0.384</b> (0.112)	0.201 (0.005)	0.248 (0.012)	0.249 (0.017)	0.254 (0.013)	0.250 (0.013)	0.244 (0.006)
$\alpha = 0.4$	$6.45 \times 10^{-5}$ ( $9.15 \times 10^{-6}$ )	<b>0.541</b> (0.155)	0.424 (0.006)	0.467 (0.007)	0.449 (0.012)	0.466 (0.011)	0.460 (0.020)	0.468 (0.015)
$\alpha = 0.6$	$1.41 \times 10^{-4}$ ( $1.74 \times 10^{-5}$ )	0.502 (0.157)	0.541 (0.010)	0.563 (0.016)	0.563 (0.016)	<b>0.568</b> (0.011)	0.559 (0.015)	0.565 (0.008)
$\alpha = 0.8$	$1.39 \times 10^{-4}$ ( $1.06 \times 10^{-6}$ )	0.576 (0.166)	0.619 (0.012)	0.620 (0.012)	0.625 (0.014)	0.624 (0.014)	<b>0.628</b> (0.007)	0.626 (0.012)
$\alpha = 1.0$	$1.47 \times 10^{-4}$ ( $7.84 \times 10^{-6}$ )	0.518 (0.169)	0.658 (0.010)	0.661 (0.007)	0.658 (0.007)	<b>0.664</b> (0.006)	0.659 (0.007)	0.653 (0.008)
Avg. Neuron Sparsity	$\ell_0$	CGES	GL	$SGL_1$	$SGL_0$	SGSCAD	$SGTL_1$	$SGL_1 - L_2$
$\alpha = 0.2$	<b>0.470</b> ( $5.97 \times 10^{-4}$ )	0.293 ( $2.61 \times 10^{-3}$ )	0.099 ( $3.77 \times 10^{-3}$ )	0.122 ( $7.25 \times 10^{-3}$ )	0.123 ( $9.71 \times 10^{-3}$ )	0.126 ( $8.39 \times 10^{-3}$ )	0.123 ( $7.86 \times 10^{-3}$ )	0.120 ( $4.93 \times 10^{-3}$ )
$\alpha = 0.4$	<b>0.494</b> ( $6.51 \times 10^{-4}$ )	0.328 ( $1.43 \times 10^{-3}$ )	0.224 ( $4.23 \times 10^{-3}$ )	0.243 ( $6.85 \times 10^{-3}$ )	0.231 (0.011)	0.241 ( $3.74 \times 10^{-3}$ )	0.238 (0.015)	0.249 (0.014)
$\alpha = 0.6$	0.198 ( $6.25 \times 10^{-5}$ )	<b>0.343</b> ( $4.82 \times 10^{-3}$ )	0.296 ( $9.94 \times 10^{-3}$ )	0.305 (0.013)	0.307 (0.014)	0.311 ( $6.32 \times 10^{-3}$ )	0.303 (0.010)	0.306 ( $9.24 \times 10^{-3}$ )
$\alpha = 0.8$	0.217 ( $2.03 \times 10^{-5}$ )	0.353 ( $3.37 \times 10^{-3}$ )	0.357 (0.012)	0.343 (0.015)	0.350 (0.011)	0.348 (0.013)	0.356 ( $4.78 \times 10^{-3}$ )	<b>0.358</b> (0.016)
$\alpha = 1.0$	0.229 ( $3.98 \times 10^{-5}$ )	0.359 ( $2.78 \times 10^{-3}$ )	<b>0.387</b> (0.010)	0.379 ( $3.75 \times 10^{-3}$ )	0.382 ( $5.85 \times 10^{-3}$ )	0.385 ( $6.37 \times 10^{-3}$ )	0.383 ( $4.66 \times 10^{-3}$ )	0.373 ( $9.97 \times 10^{-3}$ )

**Table 6.** Average test error, weight sparsity, and neuron sparsity of Resnet-40 models trained on CIFAR 10 with lowest test errors across 5 runs. Standard deviations are in parentheses.

Avg. Test Error (%)	CGES	GL	SGL <sub>1</sub>	SGL <sub>0</sub>	SGSCAD	SGTL <sub>1</sub>	SGL <sub>1</sub> – L <sub>2</sub>
α = 1.0	6.932 (0.154)	<b>6.154</b> (0.199)	6.442 (0.065)	6.456 (0.176)	6.618 (0.128)	6.500 (0.158)	6.512 (0.126)
α = 1.5	7.248 (0.145)	<b>6.504</b> (0.122)	6.850 (0.078)	7.108 (0.084)	6.948 (0.124)	6.958 (0.158)	6.820 (0.177)
α = 2.0	7.306 (0.206)	<b>6.860</b> (0.174)	7.494 (0.092)	7.642 (0.176)	7.450 (0.192)	7.388 (0.140)	7.384 (0.122)
α = 2.5	7.590 (0.148)	<b>7.298</b> (0.105)	7.760 (0.079)	8.146 (0.178)	8.026 (0.196)	8.096 (0.137)	7.968 (0.190)
α = 3.0	7.672 (0.082)	<b>7.542</b> (0.135)	8.424 (0.081)	8.740 (0.166)	8.426 (0.192)	8.624 (0.083)	8.598 (0.144)
Avg. Weight Sparsity	CGES	GL	SGL <sub>1</sub>	SGL <sub>0</sub>	SGSCAD	SGTL <sub>1</sub>	SGL <sub>1</sub> – L <sub>2</sub>
α = 1.0	<b>0.350</b> (0.009)	0.201 (0.018)	0.189 (0.007)	0.191 (0.008)	0.213 (0.015)	0.205 (0.015)	0.224 (0.016)
α = 1.5	<b>0.371</b> (0.012)	0.322 (0.008)	0.345 (0.013)	0.313 (0.008)	0.354 (0.029)	0.330 (0.020)	0.343 (0.008)
α = 2.0	0.385 (0.009)	0.431 (0.013)	0.457 (0.012)	0.422 (0.014)	<b>0.466</b> (0.015)	0.428 (0.013)	0.451 (0.012)
α = 2.5	0.386 (0.010)	0.509 (0.017)	0.525 (0.010)	0.507 (0.011)	<b>0.534</b> (0.012)	0.522 (0.026)	0.537 (0.013)
α = 3.0	0.401 (0.008)	0.551 (0.015)	<b>0.594</b> (0.009)	0.568 (0.009)	0.598 (0.012)	0.569 (0.014)	0.585 (0.006)
Avg. Neuron Sparsity	CGES	GL	SGL <sub>1</sub>	SGL <sub>0</sub>	SGSCAD	SGTL <sub>1</sub>	SGL <sub>1</sub> – L <sub>2</sub>
α = 1.0	0.035 (0.003)	0.096 (0.011)	0.087 (0.004)	0.082 (0.005)	0.102 (0.008)	0.093 (0.010)	<b>0.105</b> (0.012)
α = 1.5	0.040 (0.006)	0.154 (0.006)	0.159 (0.008)	0.144 (0.009)	<b>0.168</b> (0.013)	0.151 (0.009)	0.155 (0.004)
α = 2.0	0.048 (0.004)	0.207 (0.005)	0.203 (0.008)	0.188 (0.006)	<b>0.217</b> (0.015)	0.195 (0.009)	0.209 (0.009)
α = 2.5	0.045 (0.005)	<b>0.247</b> (0.010)	0.232 (0.010)	0.225 (0.017)	0.245 (0.011)	0.233 (0.008)	0.244 (0.006)
α = 3.0	0.048 (0.007)	<b>0.274</b> (0.012)	0.271 (0.008)	0.249 (0.004)	0.272 (0.016)	0.259 (0.008)	0.268 (0.011)

**Table 7.** Average test error, weight sparsity, and neuron sparsity of Resnet-40 models trained on CIFAR 100 with lowest test errors across 5 runs. Standard deviations are in parentheses.

Avg. Test Error (%)	CGES	$GL$	$SGL_1$	$SGL_0$	$SGSCAD$	$SGTL_1$	$SGL_1 - L_2$
$\alpha = 2.0$	30.102 (0.234)	<b>28.636</b> (0.140)	29.260 (0.306)	29.610 (0.275)	29.044 (0.155)	29.316 (0.154)	29.274 (0.249)
$\alpha = 2.5$	30.326 (0.272)	<b>29.322</b> (0.144)	30.140 (0.180)	30.454 (0.295)	30.180 (0.175)	30.426 (0.253)	30.204 (0.159)
$\alpha = 3.0$	30.378 (0.154)	<b>29.750</b> (0.258)	31.134 (0.099)	31.482 (0.361)	31.048 (0.118)	31.164 (0.236)	31.108 (0.129)
$\alpha = 3.5$	30.666 (0.267)	<b>30.588</b> (0.285)	31.966 (0.260)	32.438 (0.272)	31.930 (0.156)	31.984 (0.182)	31.822 (0.365)
$\alpha = 4.0$	<b>30.982</b> (0.277)	31.436 (0.069)	33.106 (0.281)	33.210 (0.230)	32.758 (0.279)	33.240 (0.171)	33.094 (0.219)
Avg. Weight Sparsity	CGES	$GL$	$SGL_1$	$SGL_0$	$SGSCAD$	$SGTL_1$	$SGL_1 - L_2$
$\alpha = 2.0$	<b>0.286</b> (0.002)	0.129 (0.024)	0.182 (0.018)	0.164 (0.010)	0.198 (0.012)	0.162 (0.017)	0.187 (0.015)
$\alpha = 2.5$	<b>0.299</b> (0.005)	0.233 (0.010)	0.283 (0.005)	0.251 (0.021)	0.292 (0.010)	0.271 (0.015)	0.284 (0.016)
$\alpha = 3.0$	0.303 (0.003)	0.321 (0.008)	0.365 (0.009)	0.355 (0.018)	<b>0.377</b> (0.012)	0.363 (0.023)	0.372 (0.010)
$\alpha = 3.5$	0.306 (0.004)	0.409 (0.013)	0.441 (0.014)	0.418 (0.012)	<b>0.444</b> (0.014)	0.418 (0.016)	0.442 (0.006)
$\alpha = 4.0$	0.313 (0.010)	0.456 (0.014)	<b>0.511</b> (0.015)	0.461 (0.011)	0.501 (0.013)	0.480 (0.017)	0.507 (0.012)
Avg. Neuron Sparsity	CGES	$GL$	$SGL_1$	$SGL_0$	$SGSCAD$	$SGTL_1$	$SGL_1 - L_2$
$\alpha = 2.0$	0.001 (0.001)	0.054 (0.007)	0.074 (0.007)	0.064 (0.008)	<b>0.083</b> (0.005)	0.063 (0.004)	0.078 (0.007)
$\alpha = 2.5$	0.003 (0.001)	0.092 (0.005)	0.113 (0.004)	0.093 (0.010)	<b>0.116</b> (0.005)	0.103 (0.004)	0.111 (0.005)
$\alpha = 3.0$	0.004 (0.001)	0.126 (0.004)	0.140 (0.005)	0.133 (0.007)	0.145 (0.003)	0.138 (0.009)	<b>0.146</b> (0.003)
$\alpha = 3.5$	0.002 (0.001)	0.157 (0.006)	0.166 (0.005)	0.158 (0.005)	<b>0.182</b> (0.017)	0.156 (0.004)	0.171 (0.005)
$\alpha = 4.0$	0.005 (0.002)	0.177 (0.007)	<b>0.195</b> (0.005)	0.176 (0.007)	0.193 (0.004)	0.180 (0.011)	0.193 (0.004)

**Table 8.** Average test error, weight sparsity, and neuron sparsity of WRN-28-10 models trained on CIFAR 10 with lowest test errors across 5 runs. Standard deviations are in parentheses.

Avg. Test Error (%)	CGES	GL	SGL <sub>1</sub>	SGL <sub>0</sub>	SGSCAD	SGTL <sub>1</sub>	SGL <sub>1</sub> – L <sub>2</sub>
α = 0.01	<b>3.822</b> (0.054)	4.092 (0.159)	4.050 (0.058)	4.036 (0.074)	4.004 (0.104)	3.994 (0.039)	4.152 (0.089)
α = 0.05	3.856 (0.089)	3.946 (0.106)	3.874 (0.029)	3.838 (0.067)	3.862 (0.076)	<b>3.812</b> (0.097)	3.872 (0.110)
α = 0.1	4.000 (0.076)	3.960 (0.062)	<b>3.784</b> (0.082)	3.824 (0.088)	3.832 (0.047)	3.800 (0.082)	3.792 (0.113)
α = 0.2	4.146 (0.092)	3.928 (0.115)	3.824 (0.034)	3.874 (0.093)	3.780 (0.096)	<b>3.764</b> (0.129)	3.962 (0.078)
α = 0.5	4.524 (0.090)	4.486 (0.077)	4.444 (0.086)	4.408 (0.063)	4.448 (0.084)	<b>4.340</b> (0.115)	4.382 (0.068)
Avg. Weight Sparsity	CGES	GL	SGL <sub>1</sub>	SGL <sub>0</sub>	SGSCAD	SGTL <sub>1</sub>	SGL <sub>1</sub> – L <sub>2</sub>
α = 0.01	<b>0.362</b> (0.016)	0.045 (0.001)	0.040 (0.002)	0.044 (0.002)	0.039 (0.002)	0.040 (0.001)	0.043 (0.001)
α = 0.05	<b>0.464</b> (0.003)	0.117 (0.003)	0.145 (0.006)	0.156 (0.005)	0.145 (0.007)	0.145 (0.004)	0.161 (0.006)
α = 0.1	<b>0.483</b> (0.003)	0.417 (0.005)	0.438 (0.004)	0.450 (0.005)	0.441 (0.005)	0.428 (0.004)	0.446 (0.013)
α = 0.2	0.495 (0.003)	0.673 (0.002)	0.669 (0.005)	0.672 (0.003)	0.679 (0.003)	0.666 (0.004)	<b>0.688</b> (0.003)
α = 0.5	0.503 (0.003)	<b>0.868</b> (0.001)	0.864 (0.002)	0.857 (0.001)	0.865 (0.001)	0.858 (0.002)	0.867 (0.001)
Avg. Neuron Sparsity	CGES	GL	SGL <sub>1</sub>	SGL <sub>0</sub>	SGSCAD	SGTL <sub>1</sub>	SGL <sub>1</sub> – L <sub>2</sub>
α = 0.01	<b>0.033</b> (0.002)	0.018 (0.001)	0.015 (0.001)	0.018 (0.001)	0.014 (0.001)	0.015 (0.001)	0.017 (0.001)
α = 0.02	0.050 (0.002)	0.056 (0.001)	0.068 (0.003)	0.074 (0.003)	0.069 (0.004)	0.069 (0.003)	<b>0.077</b> (0.002)
α = 0.1	0.055 (0.002)	0.178 (0.002)	0.189 (0.002)	0.190 (0.002)	0.188 (0.002)	0.182 (0.003)	<b>0.191</b> (0.006)
α = 0.2	0.059 (0.001)	0.297 (0.002)	0.294 (0.005)	0.293 (0.001)	0.299 (0.001)	0.289 (0.002)	<b>0.307</b> (0.003)
α = 0.5	0.061 (0.001)	<b>0.440</b> (0.002)	0.434 (0.002)	0.428 (0.001)	0.435 (0.001)	0.429 (0.003)	0.436 (0.001)

**Table 9.** Average test error, weight sparsity, and neuron sparsity of WRN-28-10 models trained on CIFAR 100 with lowest test errors across 5 runs. Standard deviations are in parentheses.

Avg. Test Error (%)	CGES	GL	SGL <sub>1</sub>	SGL <sub>0</sub>	SGSCAD	SGTL <sub>1</sub>	SGL <sub>1</sub> - L <sub>2</sub>
$\alpha = 0.01$	<b>18.696</b> (0.184)	19.792 (0.084)	19.494 (0.241)	19.498 (0.189)	19.368 (0.188)	19.474 (0.051)	19.632 (0.182)
$\alpha = 0.05$	<b>18.714</b> (0.203)	19.284 (0.134)	18.816 (0.141)	19.106 (0.277)	18.936 (0.085)	18.846 (0.082)	19.094 (0.272)
$\alpha = 0.1$	19.120 (0.387)	19.168 (0.067)	18.648 (0.268)	18.690 (0.181)	<b>18.446</b> (0.108)	18.680 (0.292)	18.724 (0.084)
$\alpha = 0.2$	20.298 (0.078)	18.902 (0.130)	18.440 (0.115)	18.694 (0.150)	18.502 (0.108)	<b>18.290</b> (0.107)	18.614 (0.326)
$\alpha = 0.5$	21.370 (0.259)	19.604 (0.107)	19.648 (0.203)	19.732 (0.147)	<b>19.488</b> (0.262)	19.552 (0.186)	19.732 (0.156)
Avg. Weight Sparsity	CGES	GL	SGL <sub>1</sub>	SGL <sub>0</sub>	SGSCAD	SGTL <sub>1</sub>	SGL <sub>1</sub> - L <sub>2</sub>
$\alpha = 0.01$	<b>0.281</b> (0.017)	0.013 (0.001)	0.011 (0.001)	0.013 ( $<0.001$ )	0.011 (0.001)	0.011 (0.001)	0.013 (0.001)
$\alpha = 0.05$	<b>0.412</b> (0.004)	0.014 (0.001)	0.015 (0.002)	0.017 (0.001)	0.014 (0.001)	0.015 (0.001)	0.018 (0.001)
$\alpha = 0.1$	<b>0.440</b> (0.013)	0.054 (0.002)	0.070 (0.003)	0.069 (0.001)	0.073 (0.002)	0.066 (0.002)	0.080 (0.001)
$\alpha = 0.2$	<b>0.458</b> (0.016)	0.332 (0.004)	0.356 (0.005)	0.346 (0.002)	0.355 (0.004)	0.345 (0.003)	0.361 (0.003)
$\alpha = 0.5$	0.478 (0.003)	0.697 (0.001)	0.693 (0.004)	0.685 (0.002)	<b>0.700</b> (0.002)	0.686 (0.001)	0.698 (0.002)
Avg. Neuron Sparsity	CGES	GL	SGL <sub>1</sub>	SGL <sub>0</sub>	SGSCAD	SGTL <sub>1</sub>	SGL <sub>1</sub> - L <sub>2</sub>
$\alpha = 0.01$	<b>0.008</b> (0.001)	0.002 ( $<0.001$ )	0.002 ( $<0.001$ )	0.003 ( $<0.001$ )	0.001 ( $<0.001$ )	0.002 ( $<0.001$ )	0.002 ( $<0.001$ )
$\alpha = 0.02$	<b>0.030</b> (0.001)	0.003 ( $<0.001$ )	0.005 (0.001)	0.006 ( $<0.001$ )	0.005 (0.001)	0.005 (0.001)	0.006 ( $<0.001$ )
$\alpha = 0.1$	0.037 (0.001)	0.033 (0.001)	0.044 (0.002)	0.041 ( $<0.001$ )	0.046 (0.001)	0.040 (0.001)	<b>0.050</b> (0.001)
$\alpha = 0.2$	0.043 (0.003)	0.153 (0.002)	0.157 (0.002)	0.150 (0.001)	0.157 (0.002)	0.148 (0.001)	<b>0.160</b> (0.001)
$\alpha = 0.5$	0.052 (0.001)	0.303 (0.001)	0.298 (0.001)	0.294 (0.004)	<b>0.304</b> (0.002)	0.293 (0.002)	0.303 (0.001)



**Table 10.** Average test error, weight sparsity, and neuron sparsity of  $SGL_1$ -regularized Lenet-5 models trained on MNIST after 200 epochs across 5 runs. The models are trained with different algorithms. Standard deviations are in parentheses. (SGD is stochastic gradient descent.)

Avg. Test Error (%)	direct SGD	proximal SGD	proposed
$\alpha = 0.1$	0.758 (0.029)	1.306 (0.031)	<b>0.722</b> (0.028)
$\alpha = 0.2$	0.760 (0.006)	2.954 (0.051)	<b>0.704</b> (0.031)
$\alpha = 0.3$	0.798 (0.023)	4.992 (0.161)	<b>0.732</b> (0.045)
$\alpha = 0.4$	0.836 (0.034)	7.304 (0.147)	<b>0.792</b> (0.034)
$\alpha = 0.5$	0.772 (0.019)	9.610 (0.170)	<b>0.720</b> (0.039)
Avg. Weight Sparsity	direct SGD	proximal SGD	proposed
$\alpha = 0.1$	0.935 (0.001)	<b>0.994</b> ( $<0.001$ )	0.889 (0.004)
$\alpha = 0.2$	0.951 (0.002)	<b>0.997</b> ( $<0.001$ )	0.926 (0.001)
$\alpha = 0.3$	0.960 ( $<0.001$ )	<b>0.998</b> ( $<0.001$ )	0.945 (0.001)
$\alpha = 0.4$	0.963 (0.001)	<b>0.998</b> ( $<0.001$ )	0.952 (0.001)
$\alpha = 0.5$	0.966 (0.001)	<b>0.998</b> ( $<0.001$ )	0.954 (0.002)
Avg. Neuron Sparsity	direct SGD	proximal SGD	proposed
$\alpha = 0.1$	0.735 (0.003)	<b>0.784</b> (0.004)	0.691 (0.007)
$\alpha = 0.2$	0.778 (0.004)	<b>0.902</b> (0.005)	0.754 (0.003)
$\alpha = 0.3$	0.802 (0.001)	<b>0.960</b> (0.002)	0.787 (0.003)
$\alpha = 0.4$	0.813 (0.003)	<b>0.972</b> (0.001)	0.805 (0.004)
$\alpha = 0.5$	0.821 (0.004)	<b>0.976</b> (0.002)	0.811 (0.004)

**Table 11.** Average test error, weight sparsity, and neuron sparsity of  $SGL_1$ -regularized Lenet-5 models trained on MNIST with lowest test errors across 5 runs. The models are trained with different algorithms. Standard deviations are in parentheses. (SGD is stochastic gradient descent.)

Avg. Test Error (%)	direct SGD	proximal SGD	proposed
$\alpha = 0.1$	0.594 (0.032)	1.152 (0.026)	<b>0.568</b> (0.021)
$\alpha = 0.2$	0.634 (0.031)	2.320 (0.042)	<b>0.582</b> (0.035)
$\alpha = 0.3$	0.692 (0.028)	3.360 (0.075)	<b>0.600</b> (0.030)
$\alpha = 0.4$	0.684 (0.014)	4.272 (0.051)	<b>0.652</b> (0.025)
$\alpha = 0.5$	0.636 (0.022)	5.020 (0.094)	<b>0.616</b> (0.052)
Avg. Weight Sparsity	direct SGD	proximal SGD	proposed
$\alpha = 0.1$	0.449 (0.172)	<b>0.939</b> (0.011)	0.757 (0.015)
$\alpha = 0.2$	0.531 (0.012)	<b>0.971</b> (0.005)	0.845 (0.005)
$\alpha = 0.3$	0.451 (0.217)	<b>0.992</b> ( $<0.001$ )	0.886 (0.004)
$\alpha = 0.4$	0.449 (0.213)	<b>0.989</b> (0.005)	0.896 (0.004)
$\alpha = 0.5$	0.559 (0.007)	<b>0.994</b> ( $<0.001$ )	0.905 (0.003)
Avg. Neuron Sparsity	direct SGD	proximal SGD	proposed
$\alpha = 0.1$	0.317 (0.139)	<b>0.698</b> (0.024)	0.497 (0.014)
$\alpha = 0.2$	0.444 (0.015)	<b>0.743</b> (0.021)	0.627 (0.011)
$\alpha = 0.3$	0.382 (0.185)	<b>0.863</b> (0.003)	0.697 (0.010)
$\alpha = 0.4$	0.399 (0.196)	<b>0.828</b> (0.061)	0.721 (0.008)
$\alpha = 0.5$	0.519 (0.013)	<b>0.883</b> (0.003)	0.735 (0.004)